Mathematical Biosciences and Engineering

http://www.aimspress.com/journal/MBE

MBE, 22(2): 225–259.
DOI: 10.3934/mbe.2025010
Received: 01 September 2024
Revised: 09 November 2024
Accepted: 25 November 2024
Published: 21 January 2025

Research article

Dynamics of Mpox in an HIV endemic community: A mathematical modelling approach

Andrew Omame[1,10,†], Sarafa A. Iyaniwura[2,†], Qing Han[1,3,9], Adeniyi Ebenezer[1,3,9], Nicola L. Bragazzi[4,5], Xiaoying Wang[6], Woldegebriel A. Woldegerima[1,*] and Jude D. Kong[3,7,8,9,*]

[1] Laboratory for Industrial and Applied Mathematics (LIAM), Department of Mathematics and Statistics, York University, Toronto, Ontario, Canada

[2] Theoretical Biology and Biophysics, Theoretical Division, Los Alamos National Laboratory, Los Alamos, NM 87545, USA

[3] Africa-Canada Artificial Intelligence and Data Innovation Consortium (ACADIC)

[4] Department of Clinical Pharmacy, Saarland University, Saarbrücken 66123, Germany

[5] Department of Food and Drugs, University of Parma, Parma 43125, Italy

[6] Department of Mathematics & Statistics, Trent University Peterborough, Ontario, Canada

[7] Artificial Intelligence & Mathematical Modeling Lab (AIMM Lab), Dalla Lana School of Public Health, University of Toronto, 155 College St Room 500, Toronto, ON M5T 3M7

[8] Department of Mathematics, University of Toronto, Ontario, Canada

[9] Global South Artificial Intelligence for Pandemic and Epidemic Preparedness and Response Network (AI4PEP)

[10] Department of Mathematics, Federal University of Technology, Owerri, Nigeria

† Authors contributed equally and share first authorship.

* **Correspondence:** Email: jude.kong@utoronto.ca, wassefaw@yorku.ca; Tel: +14169783868; +14379826875.

Abstract: During the 2022 monkeypox (Mpox) outbreak in non-endemic countries, sexual transmission was identified as the dominant mode of transmission, and particularly affected the community of men who have sex with men (MSM). This community experienced the highest incidence of Mpox cases, exacerbating the public health burden they already face due to the disproportionate impact of HIV. Given the simultaneous spread of HIV and Mpox within the MSM community, it is crucial to understand how these diseases interact. Specifically, since HIV is endemic within this population, understanding its influence on the spread and control of Mpox is essential. In this study, we analyze a mechanistic mathematical model of Mpox to explore the potential impact of HIV on the dynamics of Mpox within the MSM community. The model considered in this work

incorporates the transmission dynamics of the two diseases, including antiretroviral therapy (ART) for HIV. We assumed that HIV was already endemic in the population at the onset of the Mpox outbreak. Through our analysis, we derived the Mpox invasion reproduction number within an HIV-endemic setting and established the existence and local asymptotic stability of the Mpox-free equilibrium under these conditions. Furthermore, we demonstrated the existence and local asymptotic stability of an Mpox-endemic equilibrium in an HIV-endemic regime. Notably, our findings revealed that the model exhibits a backward bifurcation, a phenomenon that may not have occurred in the absence of HIV within the population. The public health significance of our results is that the presence of HIV in the MSM community could hinder efforts to control Mpox, allowing the disease to become endemic even when its invasion reproduction number is below one. Additionally, we found that Mpox might be more challenging to control in scenarios where HIV increases susceptibility to Mpox. Finally, consistent with previous studies, our analysis confirms that reducing sexual contact can be effective for controlling the spread of Mpox within the MSM community.

Keywords: HIV-Mpox co-dynamics; linear stability analysis; invasion reproduction number; bifurcation analysis; backward bifurcation; forward bifurcation

1. Introduction

Monkeypox (Mpox) is caused by the monkeypox virus [1, 2], which has its natural reservoir in animals such as monkeys and rodents [3, 4]. The virus was first identified in humans in 1970 [5, 6]. Human transmission occurs through close contact with an infected person via non-sexual (skin-to-skin) and sexual routes (anal, vaginal, or oral sex) [7]. Mpox is endemic in several African countries, including the Democratic Republic of the Congo (DRC), Ghana, Nigeria, Cameroon, and the Central African Republic (CAR) [8, 9]. Transmission in these regions is often driven by zoonotic spillover from animal hosts to humans [10, 11] or through direct human-to-human skin contact [8, 12].

In April 2022, an outbreak of Mpox occurred in multiple countries where the disease is not endemic [13, 14], thus presenting clinical and epidemiological features distinct from previous outbreaks. Notably, the virus is believed to have spread predominantly through sexual contact [15, 16]. The outbreak disproportionately affected men who have sex with men (MSM), with the highest number of cases reported within this population [17–19]. Changes in sexual behavior, alongside the roll-out of vaccination campaigns, led to a decline in Mpox cases. However, a recent resurgence in Western countries, such as Canada, and other regions, including African countries such as Burundi, Kenya, Rwanda, and Uganda, where Mpox has not been previously reported [20–22], has highlighted the need to understand the disease's dynamics in human populations. This resurgence, coupled with the emergence of a new, more virulent and deadly strain (clade I MPXV) [23, 24] which has spread even beyond the MSM population, prompted the World Health Organization (WHO) to declare it a Public Health Emergency of International Concern (PHEIC) [25, 26].

In addition to Mpox, the MSM population is disproportionately affected by several sexually transmitted infections, including the human immunodeficiency virus (HIV). By the end of 2023, approximately 39 million people were living with HIV/AIDS worldwide [27–29], with around 44% of these individuals belonging to the MSM community [30]. Despite the availability of numerous

preventive and treatment interventions, HIV continues to spread globally [31–33], with approximately 1.5 million new cases and one million HIV-related deaths annually [34, 35]. In 2022, the annual incidence rate of HIV in Canada was 4.7 per 100,000 people, with 129 HIV-related deaths reported. About 47% of those living with HIV in Canada are part of the MSM community [36, 37].

During the 2022 Mpox outbreak, 40% of the global reported cases were among people living with HIV (PWH) [17,38,39]. Notably, PWH are more susceptible to several infections, including Mpox, due to their compromised immunity [40, 41]. Given that both HIV and Mpox can be sexually transmitted and considering the high-risk sexual behaviors often associated with the MSM community [42, 43], it remains unclear whether the high prevalence of Mpox in this population is primarily due to the endemicity of HIV or other contributing factors [17, 44]. Furthermore, HIV-positive individuals are more likely to undergo diagnostic testing for Mpox relative to HIV-negative individuals [45, 46]. This underscores the importance of understanding the concurrent spread of both diseases within the MSM population.

Mathematical models that explore the co-dynamics of Mpox and HIV within a population have been studied [47–50]. Specifically, Bhunu et al. [47] analyzed a co-dynamics model for Mpox and HIV when both diseases are endemic in a general population. Their results suggest that each disease can enhance the transmission of the other. Moreover, they highlighted that both Mpox and HIV can co-exist within the population when their respective reproduction numbers are above one. In another study, Marcus et al. [48] developed an Mpox-HIV co-infection model, which they used to assess the impact of different control measures on the dynamics of both diseases. Peace et al. [49] proposed and analyzed a co-infection model for Mpox, coronavirus 2019 (COVID-19), and HIV. They considered different interventions to curtail the co-spread of the triple viral infections in a given population. Many of the aforementioned articles considered scenarios where both HIV and Mpox are endemic in a given population, which is not the case in the 2022 Mpox outbreaks, as the outbreaks occurred in populations where solely HIV was already endemic. In addition, the articles looked at the entire population without much attention to the MSM community, which is the most affected by the 2022 outbreaks. In [50], we developed a novel compartmental mathematical model to investigate the impact of HIV on the spread of Mpox in an MSM community. Unlike in the previously mentioned articles, our model mimicked the 2022-2023 Mpox outbreak, where HIV was already circulating within the MSM community at the onset of the outbreak. We showed that HIV endemicity in the MSM community can enhance the spread of Mpox. We considered scenarios were HIV infected individuals may be more susceptible to Mpox due to their compromised immune systems. Our results showed that the use antiretroviral therapy (ART) by these individuals may not be sufficient to curtail the transmission of Mpox. However, a reduction in sexual activities or a moderate use of condom, combined with ART may be beneficial to control the spread of Mpox in the population. These results were obtained by numerical simulations of our model [50].

In this study, we analyze the mathematical model developed in [50]. We aim to verify some of the results obtained therein through stability and bifurcation analyses of the model, and also study other important mathematical properties of the model, with more emphasis on understanding the impact of HIV endemicity and treatment on the spread of Mpox. To the best of our knowledge, stability analysis of the equilibria for an endemic-invasive model for HIV and Mpox has not yet been investigated in the literature. Thus, we hope to fill this gap using our existing model [50].

2. Mathematical model

We analyze the compartmental model of HIV-Mpox co-dynamics developed in [50]. The model incorporates the dynamics of individuals infected with HIV only, Mpox only, and HIV-Mpox co-infection (see Figure 1) with 12 compartments. These compartments are individuals susceptible to HIV and Mpox (S), Mpox-exposed (E_m), Mpox-infectious (I_m), Mpox-recovered (R_m), HIV-infected (I_h), HIV-infected and Mpox-exposed (E_{hm}), HIV-infected and Mpox-infectious (I_{hm}), HIV-infected and Mpox-recovered (R_{hm}), HIV-infected on ART (I_h^T), HIV-infected on ART and Mpox-exposed (E_{hm}^T), HIV-infected on ART and Mpox-infectious (I_{hm}^T), and HIV-infected on ART and Mpox-recovered (R_{hm}^T).

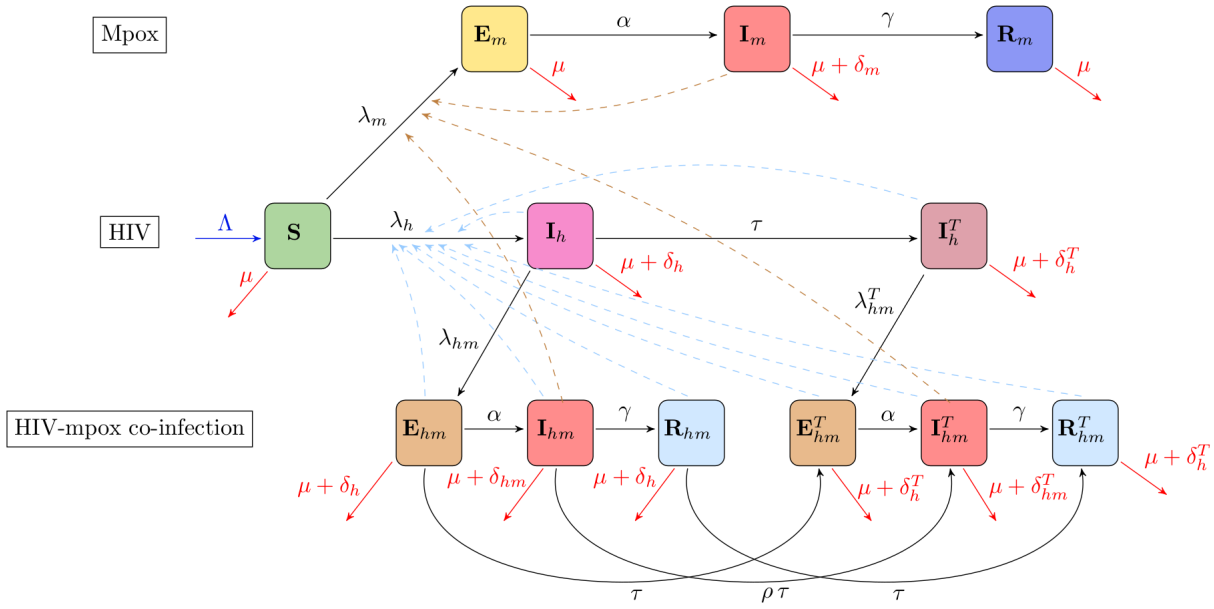

Figure 1. Schematic diagram of the co-infection model. Black solid arrows represent the transition of individuals from one stage of infection to another at the rates shown next to the arrows, red solid arrows represent the exit from the MSM community, either by death or emigration, and the blue solid arrow shows entrance into the MSM community. Blue and brown dashed arrows show the transmission of HIV and Mpox, respectively.

In this model, it is assumed that transmission of Mpox occurs at the infectious stage via sexual contacts. Individuals in the exposed stage of Mpox do not spread the infection. The current model does not capture individuals who contracted HIV while Mpox-exposed, Mpox-infectious, or Mpox-recovered. In addition, the HIV exposed stage and Mpox reinfection are not considered in the model [50]. The model incorporates HIV treatment, whereby ART usage has the likelihood to reduce susceptibility to Mpox. HIV-infected individuals not on ART may initiate treatment at any point in time while they are infected with Mpox. Since Mpox infection has the potential to make an individual visit the hospital or seek medical attention, we assume that individuals with HIV that are in the infectious stage of Mpox have a higher likelihood to initiate ART during their infection. The model assumes that an Mpox-related death only occurs at the infectious stage of the infection, and

HIV-related mortality occurs among all HIV-infected individuals, irrespective of their Mpox infection stage, though the rate is reduced for those on ART. Lastly, the model incorporates immigration into the MSM population only through the susceptible compartment (S), while an exit from the population occurs from any compartment of the model. The differential equations of the model are as follows:

$$\begin{aligned}
\frac{\mathrm{d}S}{\mathrm{d}t} &= \Lambda - (\lambda_m + \lambda_h)\, S \, - \mu S, \\
\frac{\mathrm{d}E_m}{\mathrm{d}t} &= \lambda_m S \, - (\alpha + \mu)\, E_m, \\
\frac{\mathrm{d}I_m}{\mathrm{d}t} &= \alpha E_m - (\gamma + \mu + \delta_m) I_m, \\
\frac{\mathrm{d}R_m}{\mathrm{d}t} &= \gamma I_m - \mu R_m, \\
\\
\frac{\mathrm{d}I_h}{\mathrm{d}t} &= \lambda_h S \, - \lambda_{hm} I_h - (\tau + \delta_h + \mu)\, I_h, \\
\frac{\mathrm{d}I_h^T}{\mathrm{d}t} &= \tau I_h - \lambda_{hm}^T I_h^T - \left(\delta_h^T + \mu\right) I_h^T, \\
\\
\frac{\mathrm{d}E_{hm}}{\mathrm{d}t} &= \lambda_{hm} I_h - (\tau + \alpha + \delta_h + \mu)\, E_{hm}, \\
\frac{\mathrm{d}I_{hm}}{\mathrm{d}t} &= \alpha E_{hm} - (\gamma + \rho\, \tau + \delta_{hm} + \mu)\, I_{hm}, \\
\frac{\mathrm{d}R_{hm}}{\mathrm{d}t} &= \gamma I_{hm} - (\tau + \delta_h + \mu)\, R_{hm}, \\
\frac{\mathrm{d}E_{hm}^T}{\mathrm{d}t} &= \lambda_{hm}^T\, I_h^T + \tau E_{hm} - \left(\alpha + \delta_h^T + \mu\right) E_{hm}^T, \\
\frac{\mathrm{d}I_{hm}^T}{\mathrm{d}t} &= \alpha E_{hm}^T + \rho\, \tau I_{hm} - \left(\gamma + \delta_{hm}^T + \mu\right) I_{hm}^T, \\
\frac{\mathrm{d}R_{hm}^T}{\mathrm{d}t} &= \gamma I_{hm}^T + \tau\, R_{hm} - (\delta_h^T + \mu)\, R_{hm}^T,
\end{aligned} \tag{2.1}$$

where α is the progression rate from Mpox-exposed to Mpox-infectious compartment, γ is the Mpox recovery rate, δ_m and δ_h are the Mpox and HIV related mortality rates, respectively, and δ_{hm} is the HIV or Mpox related death rate for co-infected individuals. The death rate for HIV-infected on ART is δ_h^T, while δ_{hm}^T is the mortality rate for co-infected individuals on ART. The model assumes that HIV-infected at the Mpox exposed stage or have recovered from Mpox, initiate treatment for HIV at the same rate (τ). However, individuals with HIV at the infectious stage of Mpox may start ART at a comparatively higher rate $\rho\tau$, with $\rho > 1$. Here, Λ is the immigration rate into the MSM population and μ is the rate at which people leave the MSM population, either by natural death or emigration.

The forces of infection for the transmission of Mpox (λ_m) and HIV (λ_h) are given by

$$\lambda_m = \frac{c\, p_m (1 - \nu\varepsilon)(I_m + I_{hm} + I_{hm}^T)}{N}, \tag{2.2a}$$

$$\lambda_h = \frac{c\, p_h(1-\nu\varepsilon)[I_h + E_{hm} + I_{hm} + R_{hm} + \eta(I_h^T + E_{hm}^T + I_{hm}^T + R_{hm}^T)]}{N}, \tag{2.2b}$$

where c is the average sexual contact per day and $p_m(p_h)$ is the transmission probability of Mpox (HIV) per contact. Based on these definitions, the transmission rate of Mpox (β_m) and HIV (β_h) are defined by $\beta_m = c\, p_m$ and $\beta_h = c\, p_h$, respectively. The effectiveness of intervention measures, such as condom usage, is incorporated into the model via the above forces of infection (2.2). This was performed by scaling the probability of transmission p_m and p_h, by the factor $1 - \nu\varepsilon$, where $0 \leq \nu \leq 1$ is defined as the compliance rate for condom usage and $0 < \varepsilon < 1$ is the condom efficacy. The product of these two parameters ($\xi = \nu\varepsilon$) is defined as the condom-associated preventability level. The model assumes that ART reduces the infectiousness of HIV [51, 52]. This is incorporated into the model with the help of the scaling parameter $0 \leq \eta \leq 1$ in the force of infection λ_h (2.2b). Lastly, the model assumes higher susceptibility to Mpox as a result of HIV infection [40], with those on ART having a comparatively lower increase in susceptibility [41]. This mechanism was captured in the model by scaling the force of infection λ_m by $\sigma \geq 1$ in order to obtain $\lambda_{hm} = \sigma\, \lambda_m$ for HIV-infected not on ART, and $\lambda_{hm}^T = \sigma^T \lambda_m$ with $\sigma^T \geq 1$ for HIV-infected individuals on ART, where $\sigma \geq \sigma^T$. It is important to note that $\sigma = \sigma^T = 1$ implies that there is no higher vulnerability to Mpox due to HIV infection. Additionally, the parameter σ^T may be viewed as the effectiveness of ART in reducing/preventing an increase in the vulnerability to Mpox by HIV, where $\sigma^T = 1$ implies that ART prevents increase in vulnerability, and HIV-infected persons on ART have the same susceptibility level to Mpox as those not infected with HIV. On the other hand, values of $\sigma^T > 1$ imply that HIV-infected individuals enrolled on ART have a higher vulnerability to Mpox as a result of their HIV infection. In other words, treatment with ART does not successfully prevent an increase in the vulnerability to Mpox. Our goal in this work is to study the mathematical properties of the co-infection model (2.1) as it relates to the Mpox control in the MSM community, in addition to analyzing the stability of its equilibria.

3. Model analysis

3.1. Basic features of the model

We begin our analysis of the co-dynamical model (2.1) by studying the basic properties of the model, which includes proving the non-negativity and boundedness of its solutions. These proofs are necessary for the well-posedness of the model.

3.1.1. Non-negativity of the model solutions

For the model (2.1) to be epidemiologically meaningful, it is important to show that the model solutions are non-negative. To show this, we begin by stating the following theorem.

Theorem 3.1. *Given the initial conditions*

$$\begin{aligned} &S(0) \geq 0, \quad E_m(0) \geq 0, \quad I_m(0) \geq 0, \quad R_m(0) \geq 0, \quad I_h(0) \geq 0, \quad I_h^T(0) \geq 0, \\ &E_{hm}(0) \geq 0, \quad I_{hm}(0) \geq 0, \quad R_{hm}(0) \geq 0, \quad E_{hm}^T(0) \geq 0, \quad I_{hm}^T(0) \geq 0, \quad R_{hm}^T(0) \geq 0, \end{aligned} \tag{3.1}$$

the solution

$$\Psi(t) = \left(S(t), E_m(t), I_m(t), R_m(t), I_h(t), I_h^T(t), E_{hm}(t), I_{hm}(t), R_{hm}(t), E_{hm}^T(t), I_{hm}^T(t), R_{hm}^T(t)\right) \tag{3.2}$$

of the co-infection model (2.1) *is non-negative for all time* $t > 0$.

Proof. From the first equation of the ordinary differential equation (ODE) system (2.1), we have the following:

$$\frac{\mathrm{d}S(t)}{dt} = \Lambda - (\lambda_m(t) + \lambda_h(t) + \mu)S. \tag{3.3}$$

By applying the integrating factor method on (3.3), and simplifying, we obtain the following:

$$\begin{aligned} S(t) = S(0)\exp\left[-\int_0^t (\lambda_m(u) + \lambda_h(u))\,\mathrm{d}u - \mu t\right] + \exp\left[-\int_0^t (\lambda_m(u) + \lambda_h(u))\,\mathrm{d}u - \mu t\right] \\ \times \Lambda \int_0^t \exp\left[\int_0^x (\lambda_m(u) + \lambda_h(u))\,\mathrm{d}u + \mu x\right]\mathrm{d}x \geq 0. \end{aligned}$$

Therefore, $S(t) \geq 0$ for all $t > 0$. Using a similar analysis, it can be shown that

$$\begin{aligned} &E_m(t) \geq 0, \quad I_m(t) \geq 0, \quad R_m(t) \geq 0, \quad I_h(t) \geq 0, \quad I_h^T(t) \geq 0, E_{hm}(t) \geq 0, \\ &I_{hm}(t) \geq 0, \quad R_{hm}(t) \geq 0, \quad E_{hm}^T(t) \geq 0, \quad I_{hm}^T(t) \geq 0, \quad R_{hm}^T(t) \geq 0, \end{aligned} \tag{3.4}$$

for all $t > 0$.

3.1.2. Boundedness of the model solutions

To study the boundedness of the solutions of the co-infection model (2.1), we state the following theorem.

Theorem 3.2. *The closed set* $\mathcal{D}$ *given by the following:*

$$\mathcal{D} = \left\{\left(S, E_m, I_m, R_m, I_h, I_h^T, E_{hm}, I_{hm}, R_{hm}, E_{hm}^T, I_{hm}^T, R_{hm}^T\right) \in \mathbb{R}_+^{12} \;\middle|\; N(t) \leq \frac{\Lambda}{\mu}\right\},$$

where $N(t) = S + E_m + I_m + R_m + I_h + I_h^T + E_{hm} + I_{hm} + R_{hm} + E_{hm}^T + I_{hm}^T + R_{hm}^T$ *is the total population, which is positively invariant with respect to the model* (2.1).

Proof. By adding all the equations of the ODE system (2.1), we obtain the following:

$$\begin{aligned} \frac{\mathrm{d}N(t)}{dt} = \Lambda - \mu N(t) - \Big[&\delta_m I_m(t) + \delta_h I_h(t) + \delta_h^T I_h^T(t) + \delta_h E_{hm}(t) + \delta_{hm} I_{hm}(t) + \delta_h R_{hm}(t) \\ &+ \delta_h^T E_{hm}^T(t) + \delta_{hm}^T I_{hm}^T(t) + \delta_h^T R_{hm}^T(t)\Big]. \end{aligned} \tag{3.5}$$

Since the solution of the ODE system (2.1) is non-negative (From Theorem 3.1), from (3.5), we have the following inequality:

$$\frac{\mathrm{d}N(t)}{dt} \leq \Lambda - \mu N(t). \tag{3.6}$$

Using the integrating factor method to solve (3.6), we obtain the following:

$$N(t) \leq \frac{\Lambda}{\mu} + \left(N(0) - \frac{\Lambda}{\mu}\right) e^{-\mu t}.$$

This implies that

$$\limsup_{t\to\infty} \quad N(t) \leq \frac{\Lambda}{\mu}. \tag{3.7}$$

Therefore, the total population $N(t)$ is bounded by Λ/μ as $t \to \infty$. This implies that the ODE system (2.1) has its solution in $\mathcal{D}$. Given that the solutions of this system are always positive for the positive initial conditions, as shown in Section 3.1.1, we conclude that the solutions of the model (2.1) are positively invariant.

3.2. Mpox invasion reproduction number

Next, we derive the Mpox invasion reproduction number for the co-infection model (2.1). The invasion reproduction number of a disease gives the mean number of new infections of the disease caused by one infectious individual in a population entirely susceptible to that disease, but where another disease is already endemic. Here, using the next-generation matrix approach [64], we derive the Mpox invasion reproduction number of our model in an HIV endemic regime. Let Ψ_{eh} be the Mpox-free equilibrium of the model (2.1) at an HIV endemic regime:

$$\Psi_{eh} = \left(S^*, 0, 0, 0, I_h^*, I_h^{T*}, 0, 0, 0, 0, 0, 0\right), \tag{3.8}$$

where S^*, I_h^*, and I_h^{T*} are given by the following:

$$S^* = \frac{\chi\,\Lambda}{\mho}, \qquad I_h^* = \frac{\Lambda(\delta_h^T + \mu)\left(\mathcal{R}_c^h - 1\right)}{\mho}, \qquad I_h^{T*} = \frac{\tau\Lambda\left(\mathcal{R}_c^h - 1\right)}{\mho}. \tag{3.9}$$

Here, $\mho = \varphi_h(\delta_h^T + \mu)\left(\mathcal{R}_c^h - 1\right) + \mu\chi$ with $\varphi_h = \tau + \delta_h + \mu$, $\chi = \delta_h^T + \mu + \tau$, and $\mathcal{R}_c^h$ is the control reproduction number for HIV (which is always greater than one for the existence of an HIV endemic equilibrium). It is given by the following:

$$\mathcal{R}_c^h = \frac{\Upsilon_h}{\varphi_h}\left(1 + \frac{\eta\,\tau}{\delta_h^T + \mu}\right), \tag{3.10}$$

where $\Upsilon_h = c\,p_h(1 - \nu\varepsilon)$ (see Appendix A.2 for details).

From (2.1), we consider the compartments that contribute to an Mpox infection. The equations for

these compartments are as follows:

$$\begin{aligned}
\frac{\mathrm{d}E_m}{\mathrm{d}t} &= \lambda_m S - (\alpha+\mu)\, E_m,\\
\frac{\mathrm{d}I_m}{\mathrm{d}t} &= \alpha E_m - \varphi_m I_m,\\
\frac{\mathrm{d}E_{hm}}{\mathrm{d}t} &= \lambda_{hm} I_h - \varphi_h^{\alpha}\, E_{hm},\\
\frac{\mathrm{d}I_{hm}}{\mathrm{d}t} &= \alpha\, E_{hm} - \varphi_{hm}\, I_{hm},\\
\frac{\mathrm{d}E_{hm}^T}{\mathrm{d}t} &= \lambda_{hm}^T\, I_h^T + \tau E_{hm} - \varphi_h^T\, E_{hm}^T,\\
\frac{\mathrm{d}I_{hm}^T}{\mathrm{d}t} &= \alpha E_{hm}^T + \rho\,\tau I_{hm} - \varphi_{hm}^T\, I_{hm}^T,
\end{aligned} \tag{3.11}$$

where $\varphi_m, \varphi_h^{\alpha}, \varphi_{hm}, \varphi_h^T$, and φ_{hm}^T are defined as follows:

$$\begin{gathered}
\varphi_m = \gamma + \mu + \delta_m, \qquad \varphi_h^{\alpha} = \tau + \alpha + \delta_h + \mu, \qquad \varphi_{hm} = \gamma + \rho\,\tau + \delta_{hm} + \mu,\\
\varphi_h^T = \alpha + \delta_h^T + \mu, \qquad \varphi_{hm}^T = \gamma + \delta_{hm}^T + \mu.
\end{gathered} \tag{3.12}$$

Using the above equations together with the next-generation matrix method, the Mpox invasion reproduction number is given by the following:

$$\mathcal{R}_c^{mh} = \mathcal{R}_{c,1}^{mh} + \mathcal{R}_{c,2}^{mh} + \mathcal{R}_{c,3}^{mh}\,, \tag{3.13}$$

where

$$\mathcal{R}_{c,1}^{mh} = \frac{\alpha\,\Upsilon_m}{\varphi_m\,(\alpha+\mu)\,\mathcal{R}_c^h}, \quad \mathcal{R}_{c,2}^{mh} = \frac{\sigma\alpha\,\Upsilon_m\,\mathcal{H}(\delta_h^T+\mu)\left(\mathcal{R}_c^h-1\right)}{\chi\,\varphi_h^{\alpha}\,\mathcal{R}_c^h}, \quad \mathcal{R}_{c,3}^{mh} = \frac{\alpha\,\tau\,\sigma^T\,\Upsilon_m(\delta_h^T+\mu)\left(\mathcal{R}_c^h-1\right)}{\chi\,\varphi_h^T\,\varphi_{hm}^T\,\mathcal{R}_c^h},$$

with $\mathcal{H} = 1/\varphi_{hm} + (\rho\tau)/(\varphi_{hm}\,\varphi_{hm}^T) + \tau/(\varphi_h^T\varphi_{hm}^T)$. The above invasion reproduction (3.13) defines the mean number of new Mpox infections generated by one Mpox infectious individual in a population totally susceptible to Mpox, but endemic with HIV. The terms $\mathcal{R}_{c,1}^{mh}$, $\mathcal{R}_{c,3}^{mh}$ and $\mathcal{R}_{c,3}^{mh}$ represents the mean number of new Mpox infections generated among the susceptible population, HIV-infected population not on ART, and HIV-infected population on ART, respectively. Additionally, it is important to emphasize that the Mpox invasion reproduction number ($\mathcal{R}_c^{mh}$) reflects what happens at an Mpox-free but HIV endemic regime.

3.3. Local asymptotic stability of the Mpox-free equilibrium at HIV endemic regime

In this section, we study the local asymptotic stability of the Mpox-free equilibrium (Ψ_{eh}, given in (3.8)). We begin our analysis by stating the following theorem.

Theorem 3.3. *At an HIV endemic regime, where $\mathcal{R}_c^h > 1$, the Mpox-free equilibrium of the model* (2.1) *is locally asymptotically stable whenever the Mpox invasion reproduction number $\mathcal{R}_c^{mh} < 1$ and unstable whenever $\mathcal{R}_c^{mh} > 1$.*

Proof. We consider the Jacobian matrix of the ODE system (2.1) evaluated at the Mpox-free and HIV-endemic equilibrium, Ψ_{eh}. This matrix is written in a compact form as follows:

$$J(\Psi_{eh}) = \begin{pmatrix} J_{11} & J_{12} \\ J_{21} & J_{22} \end{pmatrix}, \tag{3.14}$$

where

$$J_{11} = \begin{pmatrix} -\mu - \lambda_h^* & 0 & -\frac{\Upsilon_m}{\mathcal{R}_c^h} & 0 & -\frac{\Upsilon_h}{\mathcal{R}_c^h} & -\frac{\eta\Upsilon_h}{\mathcal{R}_c^h} \\ 0 & -(\alpha+\mu) & \frac{\Upsilon_m}{\mathcal{R}_c^h} & 0 & 0 & 0 \\ 0 & \alpha & -\varphi_m & 0 & 0 & 0 \\ 0 & 0 & \gamma & -\mu & 0 & 0 \\ \lambda_h^* & 0 & -\frac{\sigma\Upsilon_m(\delta_h^T+\mu)(\mathcal{R}_c^h-1)}{\chi\mathcal{R}_c^h} & 0 & \frac{\Upsilon_h}{\mathcal{R}_c^h} - \varphi_h & \frac{\eta\Upsilon_h}{\mathcal{R}_c^h} \\ 0 & 0 & -\frac{\sigma^T\Upsilon_m\tau(\mathcal{R}_c^h-1)}{\chi\mathcal{R}_c^h} & 0 & \tau & -(\delta_h^T+\mu) \end{pmatrix}, \tag{3.15}$$

$$J_{12} = \begin{pmatrix} -\frac{\Upsilon_h}{\mathcal{R}_c^h} & -\frac{(\Upsilon_m+\Upsilon_h)}{\mathcal{R}_c^h} & -\frac{\eta\Upsilon_h}{\mathcal{R}_c^h} & -\frac{\eta\Upsilon_h}{\mathcal{R}_c^h} & -\frac{(\Upsilon_m+\eta\Upsilon_h)}{\mathcal{R}_c^h} & -\frac{\eta\Upsilon_h}{\mathcal{R}_c^h} \\ 0 & \frac{\Upsilon_m}{\mathcal{R}_c^h} & 0 & 0 & \frac{\Upsilon_m}{\mathcal{R}_c^h} & 0 \\ 0 & 0 & 0 & 0 & 0 & 0 \\ 0 & 0 & 0 & 0 & 0 & 0 \\ \frac{\Upsilon_h}{\mathcal{R}_c^h} & \frac{\Upsilon_h}{\mathcal{R}_c^h} - \frac{\sigma\Upsilon_m(\delta_h+\mu)(\mathcal{R}_c^h-1)}{\chi\mathcal{R}_c^h} & \frac{\eta\Upsilon_h}{\mathcal{R}_c^h} & \frac{\eta\Upsilon_h}{\mathcal{R}_c^h} & \frac{\eta\Upsilon_h}{\mathcal{R}_c^h} - \frac{\Upsilon_m(\delta_h^T+\mu)(\mathcal{R}_c^h-1)}{\chi\mathcal{R}_c^h} & \frac{\eta\Upsilon_h}{\mathcal{R}_c^h} \\ 0 & -\frac{\sigma^T\Upsilon_m\tau(\mathcal{R}_c^h-1)}{\chi\mathcal{R}_c^h} & 0 & 0 & -\frac{\sigma^T\Upsilon_m\tau(\mathcal{R}_c^h-1)}{\chi\mathcal{R}_c^h} & 0 \end{pmatrix}, \tag{3.16}$$

$$J_{21} = \begin{pmatrix} 0 & 0 & \frac{\sigma\Upsilon_m(\delta_h^T+\mu)(\mathcal{R}_c^h-1)}{\chi\mathcal{R}_c^h} & 0 & 0 & 0 \\ 0 & 0 & 0 & 0 & 0 & 0 \\ 0 & 0 & 0 & 0 & 0 & 0 \\ 0 & 0 & \frac{\sigma^T\Upsilon_m\tau(\mathcal{R}_c^h-1)}{\chi\mathcal{R}_c^h} & 0 & 0 & 0 \\ 0 & 0 & 0 & 0 & 0 & 0 \\ 0 & 0 & 0 & 0 & 0 & 0 \end{pmatrix}, \tag{3.17}$$

$$J_{22} = \begin{pmatrix} -\varphi_h & \frac{\sigma\Upsilon_m(\delta_h^T+\mu)(\mathcal{R}_c^h-1)}{\chi\mathcal{R}_c^h} & 0 & 0 & \frac{\sigma\Upsilon_m(\delta_h^T+\mu)(\mathcal{R}_c^h-1)}{\chi\mathcal{R}_c^h} & 0 \\ \alpha & -\varphi_{hm} & 0 & 0 & 0 & 0 \\ 0 & \gamma & -\varphi_{hm}^T & 0 & 0 & 0 \\ \tau & \frac{\sigma^T\Upsilon_m\tau(\mathcal{R}_c^h-1)}{\chi\mathcal{R}_c^h} & 0 & -\varphi_h^T & \frac{\sigma^T\Upsilon_m\tau(\mathcal{R}_c^h-1)}{\chi\mathcal{R}_c^h} & 0 \\ 0 & \rho\tau & 0 & \alpha & -\varphi_{hm}^T & 0 \\ 0 & 0 & \tau & 0 & \gamma & -(\delta_h^T+\mu) \end{pmatrix}. \tag{3.18}$$

In these matrices, λ_h^* is the force of infection for HIV at the Mpox-free equilibrium (3.8). In addition, the total population at this equilibrium is defined as N^*. Both quantities are given by the following:

$$\lambda_h^* = \frac{\varphi_h\,(\delta_h^T+\mu)\left(\mathcal{R}_c^h-1\right)}{\chi} \qquad \text{and} \qquad N^* = \frac{\Lambda\left[\chi+(\delta_h^T+\mu)\left(\mathcal{R}_c^h-1\right)+\tau\left(\mathcal{R}_c^h-1\right)\right]}{\varphi_h(\delta_h^T+\mu)\,(\mathcal{R}_c^h-1)+\mu\chi}.$$

The Jacobian matrix $J(\Psi_{eh})$ in (3.14) has twelve eigenvalues, which are used to determine the local asymptotic stability of the Mpox-free equilibrium of the co-infection model (2.1) (at an HIV-endemic regime). The first three eigenvalues of the Jacobian matrix $J(\Psi_{eh})$ are $\Phi_1 = -\varphi_h$, $\Phi_2 = -(\delta_h^T+\mu)$, and $\Phi_3 = -\mu$. The remaining nine eigenvalues satisfy the following equations:

$$A_3\,\Phi^3 + A_2\,\Phi^2 + A_1\,\Phi + A_0 = 0 \tag{3.19}$$

and

$$\Phi^6 + B_5\,\Phi^5 + B_4\,\Phi^4 + B_3\,\Phi^3 + B_2\,\Phi^2 + B_1\,\Phi + B_0 = 0. \tag{3.20}$$

It is important to note that the polynomial Eq (3.19) is associated with the stability of the HIV endemic aspect of the equilibrium in (3.8), while the equation in (3.20) is associated with the stability of the Mpox aspect of the same equilibrium.

The coefficients of the polynomial in (3.19) are as follows:

$$\begin{aligned}
A_0 &= \varphi_h(\delta_h^T+\mu)\left(\varphi_h\,\mathcal{R}_c^h(\delta_h^T+\mu)+\mu\chi\right)\left(\mathcal{R}_c^h-1\right),\\
A_1 &= \varphi_h\,\mathcal{R}_c^h\,(\delta_h^T+\mu)\left(\mathcal{R}_c^h-1\right)\left[\varphi_h+(\delta_h^T+\mu)\right]+\mu\,\chi\left(\frac{\Upsilon_h}{(\delta_h^T+\mu)}+\mathcal{R}_c^h(\delta_h^T+\mu)\right),\\
A_2 &= \mathcal{R}_c^h\Big(\chi\,(\varphi_h+\mu)+\varphi_h(\delta_h^T+\mu)(\mathcal{R}_c^h-1)\Big)+\frac{\tau\,\eta\,\chi\,\Upsilon_h}{(\delta_h^T+\mu)},\\
A_3 &= \chi\,\mathcal{R}_c^h,
\end{aligned} \tag{3.21}$$

while those of the polynomial in (3.20) are as follows:

$$B_0 = \varphi_m\,\varphi_{hm}\,\varphi_h^{\alpha}\,\varphi_h^{T}\,\varphi_{hm}^{T}\,(\alpha+\mu)\left(1-\mathcal{R}_c^{mh}\right),$$

$$\begin{aligned}
B_1 = {} & \varphi_m\,\varphi_{hm}\,\varphi_h^{\alpha}\,\varphi_h^{T}\,(\alpha+\mu)\Big(1-[\mathcal{M}^{\mu}+(\delta_h^{T}+\mu)\mathcal{M}^{\alpha}]\Big)\\
& +\ \varphi_m\,\varphi_h^{T}\,\varphi_{hm}^{T}(\alpha+\mu)(\varphi_{hm}+\varphi_h^{\alpha})\Big[1-\left(\mathcal{M}^{\mu}+\tau\,\mathcal{M}^{T}\right)\Big]\\
& +\varphi_m\,\varphi_{hm}\,\varphi_h^{\alpha}\,\varphi_{hm}^{T}(\alpha+\mu)\left(1-\left[\mathcal{M}^{\mu}+(\delta_h^{T}+\mu)\,\mathcal{M}^{\alpha}+\frac{\tau\,(\delta_h^{T}+\mu)\,\mathcal{M}^{T}}{\varphi^{\alpha}}+\frac{\rho\,\tau(\delta_h^{T}+\mu)\mathcal{M}^{\alpha}}{\varphi_{hm}^{T}}\right]\right)\\
& +(\alpha+\mu+\varphi_m)\Big(\varphi_{hm}\,\varphi_h^{\alpha}\,\varphi_h^{T}\,\varphi_{hm}^{T}\Big)\left(1-\left[\tau\,\mathcal{M}^{T}+(\delta_h^{T}+\mu)\,\mathcal{M}^{\alpha}+\frac{\tau\,(\delta_h^{T}+\mu)\,\mathcal{M}^{T}}{\varphi^{\alpha}}+\frac{\rho\,\tau(\delta_h^{T}+\mu)\mathcal{M}^{\alpha}}{\varphi_{hm}^{T}}\right]\right),
\end{aligned}$$

$$\begin{aligned}
B_2 = {} & \varphi_m\,\varphi_{hm}\,\varphi_h^{\alpha}\,(\alpha+\mu)\Big(1-\left[\mathcal{M}^{\mu}+(\delta_h^{T}+\mu)\,\mathcal{M}^{\alpha}\right]\Big)+\varphi_m\,(\alpha+\mu)\,(1-\mathcal{M}^{\mu})\left[\,(\varphi_h^{\alpha}+\varphi_{hm})\,\mathcal{G}^{T}+\varphi_h^{T}\varphi_{hm}^{T}\right]\\
& +\varphi_{hm}\,\varphi_h^{\alpha}\Big[\varphi_h^{T}\,(\alpha+\mu)+\varphi_m\,\varphi_h^{T}\Big]\Big[1-(\delta_h^{T}+\mu)\,\mathcal{M}^{\alpha}\Big]\\
& +\varphi_h^{\alpha}\,\varphi_{hm}\Big[\varphi_{hm}^{T}\,(\alpha+\mu)+\varphi_m\,\varphi_{hm}^{T}+\varphi_h^{T}\,\varphi_{hm}^{T}\Big]\left[1-\mathcal{M}^{\alpha}\,(\delta_h^{T}+\mu)\left(1+\frac{\rho\,\tau\Upsilon_m}{\varphi_{hm}^{T}}\right)\right]\\
& +\varphi_h^{T}\,\varphi_{hm}^{T}\left(1-\tau\,\mathcal{M}^{T}\right)\Big[\varphi_m\,(\alpha+\mu)+\varphi_m\varphi_{hm}+\varphi_h^{\alpha}\varphi_{hm}\Big]\\
& +\varphi_h^{T}\,\varphi_{hm}^{T}\Big[\varphi_h^{\alpha}\,(\alpha+\mu)+\varphi_{hm}\,(\alpha+\mu)+\varphi_m\varphi_h^{\alpha}\Big]\left[1-\tau\,\mathcal{M}^{T}\left(1+\frac{(\delta_h^{T}+\mu)}{\varphi^{\alpha}}\right)\right],
\end{aligned}$$

$$\begin{aligned}
B_3 = {} & (\varphi_h^{\alpha}+\varphi_{hm})\,\mathcal{G}^{T}\Big[(\alpha+\mu)+\varphi_m\Big]+\varphi_m(\alpha+\mu)\,(1-\mathcal{M}^{\mu})\left(\varphi_h^{\alpha}+\varphi_{hm}+\mathcal{G}^{T}\right)\\
& +\varphi_{hm}\,\varphi_h^{\alpha}\Big[(\alpha+\mu)+\varphi_m+\varphi_h^{T}\Big]\Big[1-(\delta_h^{T}+\mu)\mathcal{M}^{\alpha}\Big]\\
& +\varphi_{hm}\,\varphi_h^{\alpha}\,\varphi_{hm}^{T}\Big[1-(\delta_h^{T}+\mu)\mathcal{M}^{\alpha}\left(1+\frac{\rho\,\tau}{\varphi_{hm}^{T}}\right)\Big]\\
& +\varphi_h^{T}\varphi_{hm}^{T}[(\alpha+\mu)+\mathcal{G}]\left(1-\tau\,\mathcal{M}^{T}\right)+\varphi_h^{\alpha}\,\varphi_h^{T}\,\varphi_{hm}^{T}\left[1-\tau\,\mathcal{M}^{T}\left(1+\frac{(\delta_h^{T}+\mu)}{\varphi^{\alpha}}\right)\right],
\end{aligned}$$

$$B_4 = \varphi_m\,(\alpha+\mu)\,(1-\mathcal{M}^{\mu})+\varphi_{hm}\,\varphi_h^{\alpha}\Big(1-(\delta_h^{T}+\mu)\,\mathcal{M}^{\alpha}\Big)+\varphi_h^{T}\,\varphi_{hm}^{T}\left(1-\tau\mathcal{M}^{T}\right).$$

$$B_5 = \varphi_h^{\alpha}+\mathcal{G}+\mathcal{G}^{T}+(\alpha+\mu),$$

where $\mathcal{G}=\varphi_m+\varphi_{hm}$, $\mathcal{G}^{T}=\varphi_h^{T}+\varphi_{hm}^{T}$, and $\mathcal{M}^{\alpha}$, $\mathcal{M}^{T}$, and $\mathcal{M}^{\mu}$ are defined as follows:

$$\mathcal{M}^{\alpha}=\frac{\alpha\Upsilon_m\left(\mathcal{R}_c^{h}-1\right)}{\varphi_h^{\alpha}\varphi_{hm}\chi\,\mathcal{R}_c^{h}},\qquad \mathcal{M}^{T}=\frac{\alpha\Upsilon_m\left(\mathcal{R}_c^{h}-1\right)}{\varphi_h^{T}\varphi_{hm}^{T}\chi\,\mathcal{R}_c^{h}},\quad\text{and}\quad \mathcal{M}^{\mu}=\frac{\alpha\Upsilon_m}{(\alpha+\mu)\varphi_m\mathcal{R}_c^{h}}.$$

We observe that the coefficients A_0, A_1, A_2, and A_3 are positive for $\mathcal{R}_c^{h}>1$. It can easily be shown that the coefficients B_0, B_1, B_2, B_3, B_4, and B_5 are all positive for $\mathcal{R}_c^{mh}<1$. We shall use these coefficients together with the Routh-Hurwitz criterion to determine the stability of the equilibrium Ψ_{eh}.

First, we show that the HIV-endemic regime is stable for $\mathcal{R}_c^h > 1$. The Routh-Hurwitz criterion for all the solutions of the polynomial Eq (3.19) to have negative real parts, which guarantees the local asymptotic stability of the HIV-endemic regime, is that $A_0A_3 > 0$, $A_2A_3 > 0$ and $A_1A_2 - A_0A_3 > 0$. Since A_0, A_2, and A_3 are positive when $\mathcal{R}_c^h > 1$, the conditions: $A_0A_3 > 0$, $A_2A_3 > 0$ are satisfied when $\mathcal{R}_c^h > 1$. For the last condition, we have the following:

$$\begin{aligned} A_1A_2 - A_0A_3 = &\left[\varphi_h\mathcal{R}_c^h\,(\delta_h^T+\mu)\,(\mathcal{R}_c^h-1)\Big[\varphi_h+(\delta_h^T+\mu)\Big]+\frac{\mu\chi\,\Upsilon_h}{(\delta_h^T+\mu)}+\mu\chi\,(\delta_h^T+\mu)\,\mathcal{R}_c^h\right]\\ &\times\left[\varphi_h\,\mathcal{R}_c^h\,(\delta_h^T+\mu)(\mathcal{R}_c^h-1)+\frac{\mu\chi\,\Upsilon_h}{(\delta_h^T+\mu)}+\mu\chi\,(\delta_h^T+\mu)\right]\\ &+\varphi_h\chi\,\mathcal{R}_c^h\left[\mu\chi(\delta_h^T+\mu)+\left(\varphi_h^2\,\mathcal{R}_c^h\,(\delta_h^T+\mu)(\mathcal{R}_c^h-1)+\frac{\mu\chi\,\Upsilon_h}{(\delta_h^T+\mu)}\right)\right], \end{aligned}$$

which is also positive for $\mathcal{R}_c^h > 1$. Therefore, the HIV-endemic regime is stable for $\mathcal{R}_c^h > 1$

For the Mpox-free aspect of the equilibrium (3.8), we consider the Routh-Hurwitz criterion for all roots of a polynomial of degree six to have a negative real part. This criterion requires that the determinants of the Hurtwitz matrices associated with the characteristic Eq (3.20) are positive [65,66]. That is,

$$Det\begin{pmatrix} B_5 & B_3 & B_1\\ 1 & B_4 & B_2\\ 0 & B_5 & B_3\end{pmatrix} > 0 \quad \textbf{and} \quad Det\begin{pmatrix} B_5 & B_3 & B_1 & 0 & 0\\ 1 & B_4 & B_2 & B_0 & 0\\ 0 & B_5 & B_3 & B_1 & 0\\ 0 & 1 & B_4 & B_2 & B_0\\ 0 & 0 & B_5 & B_3 & B_1\end{pmatrix} > 0. \tag{3.22}$$

It can be verified that the conditions in (3.22) are satisfied when $\mathcal{R}_c^{mh} < 1$. However, we do not show the details here due to the length of the resulting expressions. Based on Routh-Hurwitz criterion, we are guaranteed that the roots of the polynomial equations in (3.19) and (3.20) have negative real parts when $\mathcal{R}_c^h > 1$ and $\mathcal{R}_c^{mh} < 1$, respectively. Additionally, these results guarantee the local asymptotic stability of the Mpox-free equilibrium of the model (2.1) at an HIV-endemic regime when $\mathcal{R}_c^{mh} < 1$.

To prove the instability of the Mpox-free equilibrium Ψ_{eh} when $\mathcal{R}_c^{mh} > 1$ (at an HIV-endemic regime), it is sufficient to show that one of the Routh-Hurwitz criteria required for the stability of this equilibrium is not satisfied for $\mathcal{R}_c^{mh} > 1$. Since the stability of the Mpox free equilibrium requires that $B_0 > 0$, we observe that this condition is not satisfied when $\mathcal{R}_c^{mh} > 1$. Therefore, the Mpox-free equilibrium is unstable for $\mathcal{R}_c^{mh} > 1$. Thus, we conclude that, at an HIV-endemic regime, where $\mathcal{R}_c^h > 1$, the Mpox-free equilibrium, Ψ_{eh}, of the model (2.1) is locally asymptotically stable whenever $\mathcal{R}_c^{mh} < 1$ and unstable whenever $\mathcal{R}_c^{mh} > 1$.

3.4. Mpox-endemic equilibrium at HIV-endemic regime

Several models have been formulated to independently investigate the dynamics of Mpox and HIV [67–70]. For many of these models, the existence and stability of Mpox-endemic equilibrium (in the absence of HIV) were studied [67, 68], and similarly for HIV [69, 70]. In this section, we study the existence and stability of the Mpox-endemic equilibrium of the model (2.1) at an HIV-endemic regime.

Specifically, we aim to have a good understanding of the impact of HIV endemicity on the stability of Mpox-endemic equilibrium.

Since only a few Mpox-induced deaths were reported during the 2022 outbreak [71] and HIV treatment with ART has significantly reduced deaths from HIV [36, 72], we consider a scenario of our model, where the disease-induced death for both Mpox and HIV are negligible. In other words, we set the Mpox and HIV death rates to zero in our model (i.e., $\delta_m = \delta_h = \delta_{hm} = \delta_h^T = \delta_{hm}^T = 0$) in Eq (2.1). In this case, the total population becomes constant ($N = \Lambda/\mu$) and the Mpox and HIV transmission rates are $\bar{\beta}_m = (c\, p_m\, \mu)/\Lambda$ and $\bar{\beta}_h = (c\, p_h\, \mu)/\Lambda$, respectively.

Let Ψ_e be an arbitrary Mpox-endemic equilibrium, given by the following:

$$\Psi_e = \left(S^e, E_m^e, I_m^e, R_m^e, I_h^e, I_h^{Te}, E_{hm}^e, I_{hm}^e, R_{hm}^e, E_{hm}^{Te}, I_{hm}^{Te}, R_{hm}^{Te}\right), \tag{3.23}$$

and let λ_m^e and λ_h^e, given by the following:

$$\lambda_m^e = \bar{\beta}_m(1-\nu\varepsilon)(I_m^e + I_{hm}^e + I_{hm}^{Te}) \qquad \text{and} \qquad \lambda_h^e = \bar{\beta}_h(1-\nu\varepsilon)(I_h^e + \eta I_h^{Te}), \tag{3.24}$$

be the forces of infection for Mpox and HIV, respectively, at the Mpox-endemic equilibrium. The equilibrium solutions of the model (2.1), without disease-induced deaths at an Mpox-endemic equilibrium are given by the following:

$$S^e = \frac{\Lambda}{\hat{\lambda}^e}, \qquad E_m^e = \frac{\lambda_m^e \Lambda}{(\alpha+\mu)\,\hat{\lambda}^e}, \qquad I_m^e = \frac{\alpha\lambda_m^e\Lambda}{(\alpha+\mu)\,(\gamma+\mu)\,\hat{\lambda}^e}, \qquad R_m^e = \frac{\alpha\gamma\lambda_m^e\Lambda}{\mu\,(\alpha+\mu)\,(\gamma+\mu)\,\hat{\lambda}^e},$$

$$I_h^e = \frac{\lambda_h^e\Lambda}{\hat{\lambda}_{hm}^e\hat{\lambda}^e}, \qquad I_h^{Te} = \frac{\tau\lambda_h^e\Lambda}{\left(\lambda_{hm}^{Te}+\mu\right)\hat{\lambda}^e\,\hat{\lambda}_{hm}^e}, \qquad E_{hm}^e = \frac{\sigma\lambda_m^e\lambda_h^e\Lambda}{\hat{\varphi}_h^\alpha\,\hat{\lambda}^e\,\hat{\lambda}_{hm}^e}, \qquad I_{hm}^e = \frac{\alpha\sigma\lambda_m^e\lambda_h^e\Lambda}{\hat{\varphi}_h^\alpha\,\hat{\varphi}_{hm}\,\hat{\lambda}^e\,\hat{\lambda}_{hm}^e},$$

$$R_{hm}^e = \frac{\alpha\,\gamma\,\sigma\lambda_m^e\,\lambda_h^e\,\Lambda}{\hat{\varphi}_h^\alpha\,\hat{\varphi}_{hm}\,(\tau+\mu)\;\hat{\lambda}^e\,\hat{\lambda}_{hm}^e}, \qquad E_{hm}^{Te} = \frac{\sigma\,\tau\,\lambda_m^e\,\lambda_h^e\,\Lambda}{\hat{\varphi}_h^\alpha\,(\alpha+\mu)\,\hat{\lambda}^e\,\hat{\lambda}_{hm}^e}\left(\frac{\sigma^T a}{\left(\lambda_{hm}^{Te}+\mu\right)} + \frac{\sigma}{\hat{\varphi}_h^\alpha}\right),$$

$$I_{hm}^{Te} = \frac{\tau\,\alpha\,\lambda_m^e\,\lambda_h^e\,\Lambda}{\hat{\lambda}^e\,\hat{\lambda}_{hm}^e(\gamma+\mu)}\left(\frac{\sigma^T}{\left(\lambda_{hm}^{Te}+\mu\right)(\alpha+\mu)} + \frac{\sigma}{\hat{\varphi}_h^\alpha\,(\alpha+\mu)} + \frac{\sigma\,\rho}{\hat{\varphi}_h^\alpha\,\hat{\varphi}_{hm}}\right),$$

$$R_{hm}^{Te} = \frac{\tau\,\alpha\,\gamma\,\lambda_m^e\,\lambda_h^e\,\Lambda}{\mu\,\hat{\lambda}^e\,\hat{\lambda}_{hm}^e}\left[\frac{1}{(\alpha+\mu)(\gamma+\mu)}\left(\frac{\sigma^T}{\left(\lambda_{hm}^{Te}+\mu\right)} + \frac{\sigma}{\hat{\lambda}_{hm}^e}\right) + \frac{\sigma\rho}{\hat{\varphi}_h^\alpha\,\hat{\varphi}_{hm}(\gamma+\mu)} + \frac{\sigma}{(\tau+\mu)\,\hat{\varphi}_h^\alpha\,\hat{\varphi}_{hm}}\right], \tag{3.25}$$

where $\hat{\lambda}^e, \hat{\lambda}_{hm}^e, \hat{\varphi}_h^\alpha$, and $\hat{\varphi}_{hm}$ are defined as follows:

$$\hat{\lambda}^e = \lambda_m^e + \lambda_h^e + \mu, \qquad \hat{\lambda}_{hm}^e = \lambda_{hm}^e + \tau + \mu, \qquad \hat{\varphi}_h^\alpha = \tau + \alpha + \mu, \qquad \hat{\varphi}_{hm} = \gamma + \rho\,\tau + \mu.$$

By substituting the equilibrium solutions in (3.25) into the force of infection for Mpox in (3.24), we construct the following polynomial:

$$a_3(\lambda_m^e)^3 + a_2(\lambda_m^e)^2 + a_1\lambda_m^e + a_0 = 0, \tag{3.26}$$

whose coefficients are given by the following:

$$
\begin{aligned}
a_0 &= \varrho\,\mu^2\,(\tau+\mu)\bar{\mathcal{R}}_c^h\left(1-\bar{\mathcal{R}}_c^{mh}\right),\\
a_1 &= \varrho\,\mu\left[\left(\sigma\,\mu+\sigma^T\,(\tau+\mu)\right)\bar{\mathcal{R}}_c^h\,(1-\mathcal{W})+(\tau+\mu)\left(1-\frac{\sigma\,\sigma^T\alpha\bar{\beta}_m(1-\nu\,\varepsilon)\Lambda\,\mu\,\left(\bar{\mathcal{R}}_c^h-1\right)\hat{\mathcal{H}}}{(\tau+\mu)\hat{\varphi}_h^{\alpha}}\right)\right],\\
a_2 &= \varrho\Big[\left(\sigma\mu+\sigma^T(\tau+\mu)\right)+\sigma\,\sigma^T\,\mu\,\bar{\mathcal{R}}_c^h\,(1-\mathcal{W})\Big],\\
a_3 &= \varrho\,\sigma\,\sigma^T.
\end{aligned}
\tag{3.27}
$$

Here, $\varrho=\hat{\varphi}_h^{\alpha}\,(\alpha+\mu)^2(\gamma+\mu)^2(\gamma+\rho\tau+\mu)$, and $\hat{\mathcal{H}}$ and $\mathcal{W}$ are given by the following:

$$
\hat{\mathcal{H}}=\frac{1}{\gamma+\rho\tau+\mu}+\frac{\rho\,\tau}{(\gamma+\rho\,\tau+\mu)\,(\gamma+\mu)}+\frac{\tau}{(\alpha+\mu)(\gamma+\mu)}\qquad\text{and}\qquad\mathcal{W}=\frac{\bar{\beta}_m(1-\nu\,\varepsilon)\,\alpha\,\Lambda}{(\alpha+\mu)(\gamma+\mu)\,\mu\,\bar{\mathcal{R}}_c^h}.
$$

The components of the Mpox-endemic equilibrium in (3.23) are obtained from the polynomial in (3.26) upon solving for λ_m^e and substituting the positive values of λ_m^e into the expressions in (3.25). It is important to note that the coefficients of polynomial (3.26) determine the existence of the Mpox-endemic equilibrium. We observe from (3.27) that the coefficient a_3 is always positive, and a_0 is positive (negative) if the Mpox invasion reproduction number $\bar{\mathcal{R}}_c^{mh}$ is less (greater) than one. It can easily be verified that $a_2>0$ when the Mpox invasion reproduction number is less than one ($\bar{\mathcal{R}}_c^{mh}<1$). This shows that the existence of the Mpox-endemic equilibrium depends on the sign of a_1. We summarize the potential scenarios for the existence of this equilibrium in Theorem 3.4.

Theorem 3.4. *The co-infection model* (2.1) *(without disease-induced deaths for both Mpox and HIV) at an HIV-endemic regime has the following:*

(i) two Mpox endemic equilibria if $\bar{\mathcal{R}}_c^{mh}<1$ *and* $a_1<0$*;*
(ii) a unique Mpox endemic equilibrium if $\bar{\mathcal{R}}_c^{mh}>1$ *and* $a_1>0$, $a_2<0$*; and*
(iii) no Mpox endemic equilibrium if $\bar{\mathcal{R}}_c^{mh}<1$ *and* $a_1>0$.

Item (i) of Theorem 3.4 suggests the possibility of the model exhibiting a backward bifurcation, in which case, there will be two positive Mpox-endemic equilibria when $\bar{\mathcal{R}}_c^{mh}<1$. We summarize this result in the theorem below.

Theorem 3.5. *The co-infection model* (2.1) *(without disease-induced deaths for both Mpox and HIV) at an HIV-endemic regime will exhibit a backward bifurcation (co-existence of a stable Mpox-free equilibrium and a stable Mpox-endemic equilibrium when* $\bar{\mathcal{R}}_c^{mh}<1$*) whenever the following condition holds:*

$$
\sigma^c>\frac{\hat{\varphi}_h^{\alpha}\left[\left(\sigma\,\mu+\sigma^T\,(\tau+\mu)\right)\bar{\mathcal{R}}_c^h\,(1-\mathcal{W})+(\tau+\mu)\right]}{\sigma^T\,\alpha\,\mu\,\bar{\beta}_m\;\Lambda\,(1-\nu\,\varepsilon)\left(\bar{\mathcal{R}}_c^h-1\right)\hat{\mathcal{H}}},
\tag{3.28}
$$

where $\nu\varepsilon<1$ and $\bar{\mathcal{R}}_c^h>1$.

Remark 3.1. *It is important to highlight that although the local stability analysis of both the Mpox-free and Mpox-endemic equilibria around the HIV endemic regime of the model* (2.1) *have been used to obtain the key analytical results of the current study, the global stability analysis can also be obtained for a special case of the model* (2.1)*, where the dynamics of the two diseases are decoupled. This special case of the model corresponds to a scenario where both HIV and Mpox independently circulate within the population without co-infection. However, in the present study, this scenario is not qualitatively analyzed, as it is almost an unrealistic reflection of real-world scenarios where such a decoupling is unlikely. However, a future study shall aim to explore the global dynamics of the coupled system using some novel techniques.*

4. Model simulation

We numerically generate the bifurcation diagram for the model (2.1) by solving the polynomial Eq (3.26) using MATLAB, version R2024a [73], for different values of the invasion reproduction number of Mpox $\bar{\mathcal{R}}_c^{mh}$. The remaining model parameters are fixed at the values shown in Table 1, except otherwise stated in the figure captions. We set the HIV control reproduction number $\bar{\mathcal{R}}_c^{h} = 1.2325$, such that HIV is already endemic in the population at the beginning and during the Mpox outbreak. Our aim is to obtain solutions of the cubic polynomial Eq (3.26) when $\bar{\mathcal{R}}_c^{mh}$ is varied. These solutions will be used to determine the existence and stability of the endemic equilibrium of the model (2.1). It is important to note that $a_1 < 0$ based on our parameters. When $\bar{\mathcal{R}}_c^{mh} < 1$, we found that the polynomial equation has two positive solutions (the third solution has negative real part). This suggests the existence of a backward bifurcation based on item (i) of Theorem 3.4. Note that this bifurcation only exists when the inequality in Theorem 3.5 holds. For $\bar{\mathcal{R}}_c^{mh} > 1$, the polynomial Eq (3.26) has only one solution with a positive real part, which suggests the existence of a stable endemic equilibrium. The root (λ_m^e) of the polynomial equation is plotted with respect to the invasion reproduction number of Mpox $\bar{\mathcal{R}}_c^{mh}$ as our bifurcation diagram.

Figure 2 shows the existence of a backward bifurcation for the co-infection model (2.1). The bifurcation diagrams in this figure are plotted for different values of the parameters σ and σ^T, representing increase in vulnerability to Mpox as a result of HIV infection for HIV-infected individuals not on ART (I_h) and those on ART (I_h^T), respectively. The occurrence of a backward bifurcation in an epidemic model implies that the requirement associated with the reproduction number less than one, although still necessary, is not sufficient for the control of the disease [74, 75]. Thus, the control of the disease becomes more difficult in the population. This feature is usually signaled by the appearance of two endemic equilibria co-existing with a stable disease-free equilibrium whenever the threshold quantity, called the reproduction number, is below one. In the left panel of Figure 2, we present our result for scenarios where an HIV infection leads to a higher vulnerability to Mpox. We assume this increase in susceptibility in our model to account for the potential compromise in the immune systems of those infected with HIV. We observe that the endemic equilibrium lobe in the bifurcation diagrams presented in this figure increase as the susceptibility of HIV-infected individuals to Mpox increases. These results suggest that an increase in the vulnerability to Mpox for HIV-infected individuals in the population will negatively impact Mpox control in the population. To identify the main factor contributing to the existence of a backward bifurcation, we consider a scenario where HIV does not increase vulnerability to Mpox (i.e.,

$\sigma = \sigma^T = 1$) with result shown in the right panel of Figure 2. We observe that the backward bifurcation still exists for this scenario, thus suggesting that the existence of a backward bifurcation is not due to increase in the susceptibility to Mpox for those infected with HIV.

Table 1. Model parameters, descriptions, and values. $CN_{pop} = 38,929,902$ is the total Canadian population at the onset of the 2022-2023 Mpox outbreak [53].

Parameter	Description	Value	Source
p_m	Transmission probability of Mpox per sexual contact	0.19	[54–58]
c	Average per-capita sexual contact per day	0.85 day^{-1}	[54]
p_h	HIV transmission probability per contact	0.012	[32, 59]
ν	Compliance rate for condom usage	0.61	[60]
ε	Efficacy of condom	0.92	[61]
μ	Rate of exiting the MSM population	0.003 day^{-1}	[62]
N	Total population	4% of CN_{pop}	[53]
Λ	Recruitment rate	$N \times \mu$ day^{-1}	[53, 62]
γ	Recovery rate from Mpox	$\frac{1}{14}$ day^{-1}	[55]
α	Rate of transitioning from Mpox-exposed to Mpox-infectious stage	$\frac{1}{8.5}$ day^{-1}	[63]
τ	ART enrollment rate	0.035	[32, 59]
ρ	Modification parameter for higher rate of ART enrollment among co-infected individuals	1.2	Assumed
δ_m	Mpox-related mortality rate	0	[71]
δ_h	HIV-related mortality rate for those not enrolled on ART	0.007 day^{-1}	[59]
δ_{hm}	HIV- or Mpox-related mortality rate among co-infected individuals that are not enrolled yet on ART	0.007 day^{-1}	[59]
δ_h^T	HIV-related mortality rate among individuals that are enrolled on ART	0 day^{-1}	[59]
δ_{hm}^T	HIV- or Mpox-related mortality rate among co-infected individuals that are enrolled on ART	0 day^{-1}	[59]
σ	Modification parameter for higher susceptibility to Mpox as a result of HIV infection	varied	[40]
σ^T	Modification parameter for higher susceptibility to Mpox as a result of HIV infection for individuals that are enrolled on ART	varied	[41]
η	Modification parameter for reduced infectivity of individuals that are enrolled on ART	0.15	[59]
$\Omega = \frac{I_h^{T*}}{I_h^* + I_h^{T*}}$	The fraction of HIV-infected population already on ART at the onset of Mpox outbreak	0.75	[32]

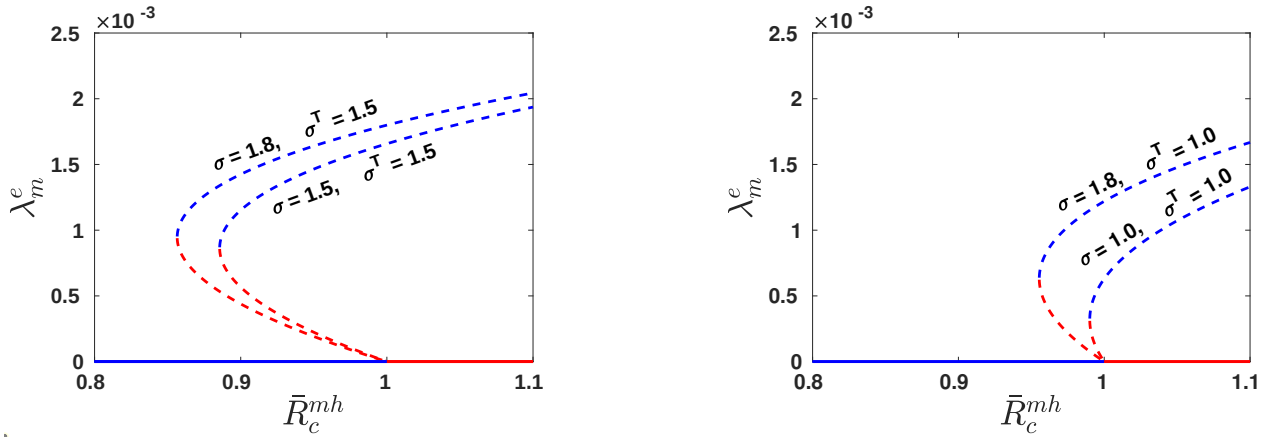

Figure 2. Existence of a backward bifurcation. Bifurcation diagrams for the co-infection model (2.1) plotted in terms of the Mpox invasion reproduction number ($\mathcal{R}_c^{mh}$) and the force of infection (λ_m^e) for different values of σ and σ^T. Blue and red dashed lines represent stable and unstable Mpox-endemic equilibrium, respectively. Solid blue and red lines represent stable and unstable Mpox-free equilibrium, respectively. Parameters are given in Table 1 with corresponding HIV control reproduction number $\bar{\mathcal{R}}_c^h = 1.2325$.

We hypothesize that the existence of the backward bifurcation shown in Figure 2 is due to the co-circulation of Mpox and HIV, and more importantly, the endemicity of HIV in the population during the Mpox outbreak. To verify this, we set $\sigma = 0$ and $\sigma^T = 0$ to mathematically decouple the infection process of Mpox and HIV in our model. As a result, the cubic polynomial Eq (3.26) reduces to the following:

$$\varrho\,\mu\,(\tau+\mu)\lambda_m^e + \varrho\,\mu^2\,(\tau+\mu)\bar{\mathcal{R}}_c^h\left(1-\bar{\mathcal{R}}_c^{mh}|_{\sigma=\sigma^T=0}\right) = 0. \tag{4.1}$$

This implies no sign change (in the sense of Descartes' rule of signs [76]) in the coefficients of the polynomial for $\bar{\mathcal{R}}_c^{mh}|_{\sigma=\sigma^T=0} < 1$, since all the coefficients in this case are positive, which completely rules out the possibility of a backward bifurcation in the model. Using the reduced polynomial equation in (4.1), we generate the bifurcation diagram in Figure 3, which gives a forward bifurcation as predicted.

To gain an intuition for the existence of the forward bifurcation shown in Figure 3, when $\sigma = \sigma^T = 0$, we consider the Mpox force of infection for individuals infected with HIV who are not on ART ($\lambda_{hm} = \sigma\,\lambda_m$) and those on ART ($\lambda_{hm}^T = \sigma^T\lambda_m$), where λ_m is the Mpox force of infection for the general susceptible population. We observe that $\lambda_{hm} = 0$ and $\lambda_{hm}^T = 0$ when $\sigma = 0$ and $\sigma^T = 0$, respectively (i.e., there is no co-infection in this case). In addition, the HIV and Mpox dynamics decouple under this assumption. As a result, the bifurcation diagram in Figure 3 represents the dynamics of a model for the sole spread of Mpox in the population (no HIV infections). Additionally, this observation aligns with the results in Appendices A.1 and A.2, where the separate analyses of Mpox and HIV submodels also reveal the absence of a backward bifurcation.

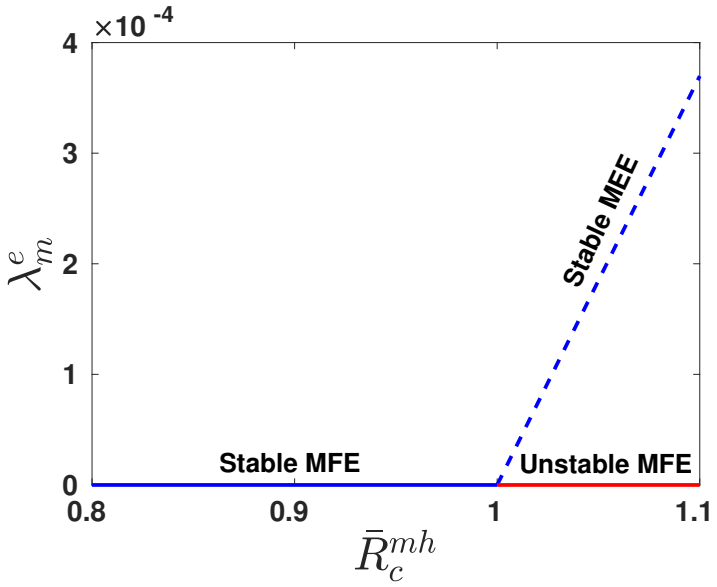

Figure 3. Forward bifurcation for when $\sigma = \sigma^T = 0$. Bifurcation diagrams for the model (2.1) presented in terms of the Mpox invasion reproduction number ($\mathcal{R}_c^{mh}$) and the Mpox force of infection (λ_m^e) when $\sigma = \sigma^T = 0$. Blue dashed line shows a stable Mpox-endemic equilibrium (MEE), solid blue line shows a stable Mpox free equilibrium (MFE), and solid red line shows an unstable Mpox free equilibrium (MFE). Parameters are given in Table 1 with the corresponding HIV control reproduction number $\bar{\mathcal{R}}_c^h = 1.2325$.

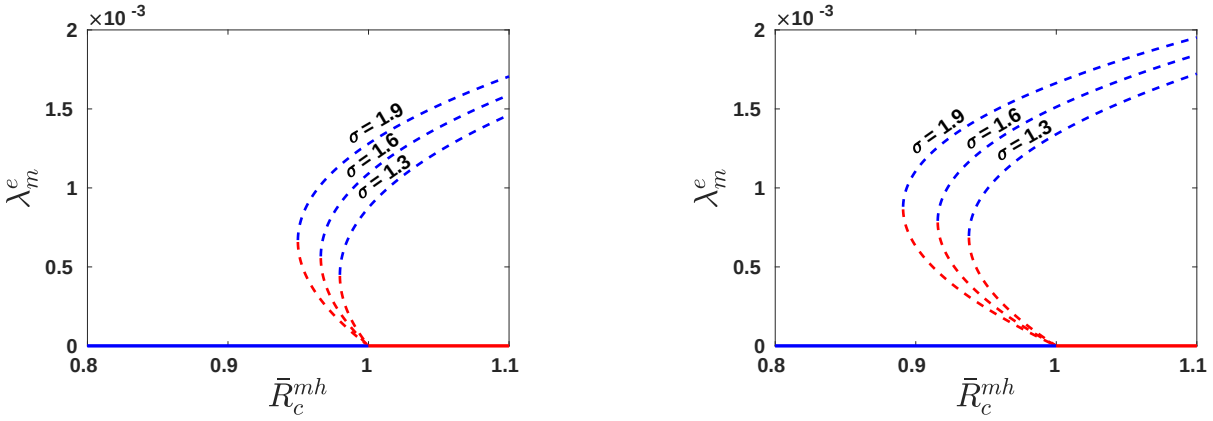

Figure 4. Effect of increased susceptibility to Mpox due to HIV. Bifurcation diagrams for the co-infection model (2.1) presented in terms of the Mpox invasion reproduction number ($\mathcal{R}_c^{mh}$) and the Mpox force of infection (λ_m^e) for different values of σ and σ^T. Blue and red dashed lines represent stable and unstable Mpox-endemic equilibrium, respectively. Solid blue and red lines represent stable and unstable Mpox-free equilibrium, respectively. Left panel: $\sigma^T = 1.0$. Right panel: $\sigma^T = 1.3$. Parameters are given in Table 1 with the corresponding HIV control reproduction number $\bar{\mathcal{R}}_c^h = 1.2325$.

The results in Figure 4 emphasize the importance of an HIV treatment in the control of Mpox. The results in the left panel of this figure were generated using $\sigma^T = 1.0$. In terms of HIV treatment, this implies that HIV the treatment is effective enough to prevent HIV-infected individuals on treatment from becoming more susceptible to Mpox. Comparing the results in this panel to those in the right panel, which were generated with the same values of σ but with $\sigma^T = 1.3$ (which can be interpreted as HIV treatment being not effective enough to prevent an increase in the vulnerability to Mpox), we observe that the endemic equilibrium lobe is larger when $\sigma^T = 1.3$ compared to when $\sigma^T = 1.0$. This suggests that Mpox will be more difficult to control when the HIV treatment is not effective enough to reduce the susceptibility of those on ART. Although, we interpreted this result in terms of the treatment not being effective, the results may also be interpreted as individuals not being consistent with taking their medication, since ART has been shown to significantly reduce the viral levels when taken consistently as required [77]. These results highlight the potential consequence of HIV treatments on the control of Mpox spread.

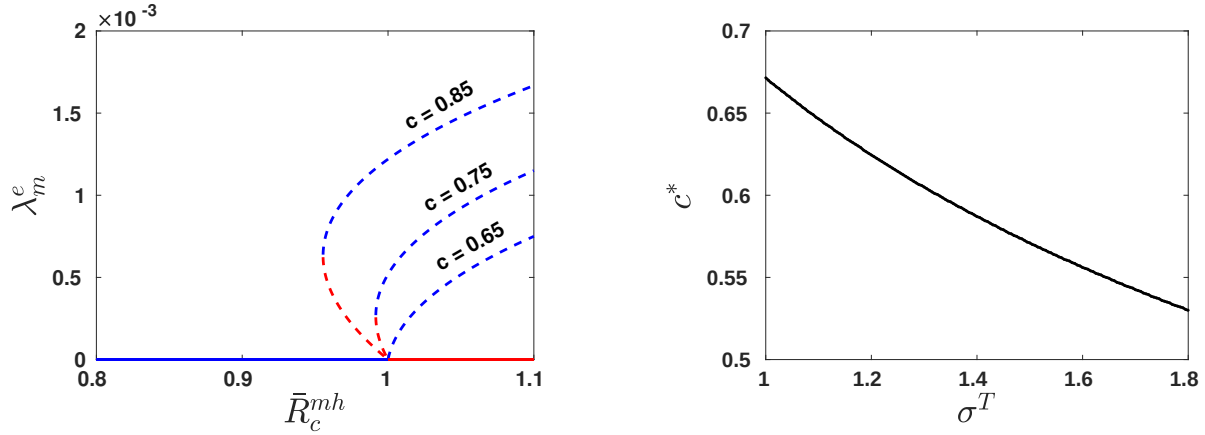

Figure 5. Effect of sexual contact and HIV treatment on the Mpox dynamics. Left panel: Bifurcation diagrams for the model (2.1) presented in terms of the Mpox invasion reproduction number ($\mathcal{R}_c^{mh}$) and the force of infection (λ_m^e) for varying values of the sexual contact rate c when $\sigma = 1.8$ and $\sigma^T = 1.0$. Blue dashed line shows a stable Mpox-endemic equilibrium, while red dashed line shows an unstable Mpox-endemic equilibrium. Solid blue and red lines show stable and unstable Mpox-free equilibrium, respectively. Right panel: The critical sexual contact rate (c^*) at which a backward bifurcation switches to a forward bifurcation for different values of σ^T. Recall, σ^T is the increase in vulnerability to Mpox for HIV infected individuals on ART. The parameters are given in Table 1.

Lastly, we study the potential effect of sexual contact on the control of Mpox in the MSM population. Given the high level of sexual activities associated with the MSM community [78, 79], it is important to investigate the effect of sexual contacts on the spread of Mpox in the community. In Figures 2–4, we have used a fixed sexual contact rate, $c = 0.85$. To have a good understanding of the effect of this parameter on the model dynamics, we vary its value while the remaining model parameters are fixed (Figure 5, left panel). The result from this analysis shows a transition from a forward bifurcation to a backward bifurcation as the sexual contact rate increases, which suggest that Mpox will be more difficult to control in the MSM population as the sexual contacts increase in the

population. Here, we assume that HIV increases the vulnerability to Mpox in HIV-infected individuals not on ART ($\sigma = 1.8$) and has no effect on the susceptibility of those on treatment ($\sigma^T = 1.0$). This assumption can also be interpreted as the HIV treatment being effective enough to prevent those on ART from having an increased vulnerability to Mpox like those not on ART. To have a good understanding of the the impact of sexual contacts and HIV treatment on Mpox control, we computed the critical sexual contact rate (c^*) at which there was a switch from a backward bifurcation to a forward bifurcation (vice versa) for different values of σ^T. Our result shows that c^* decreases non-linearly as σ^T increases (Figure 5, right panel), which signifies that the critical contact rate at which the transition from a backward to a forward bifurcation happens to decrease as the vulnerability to Mpox for HIV infected individuals on ART increases.

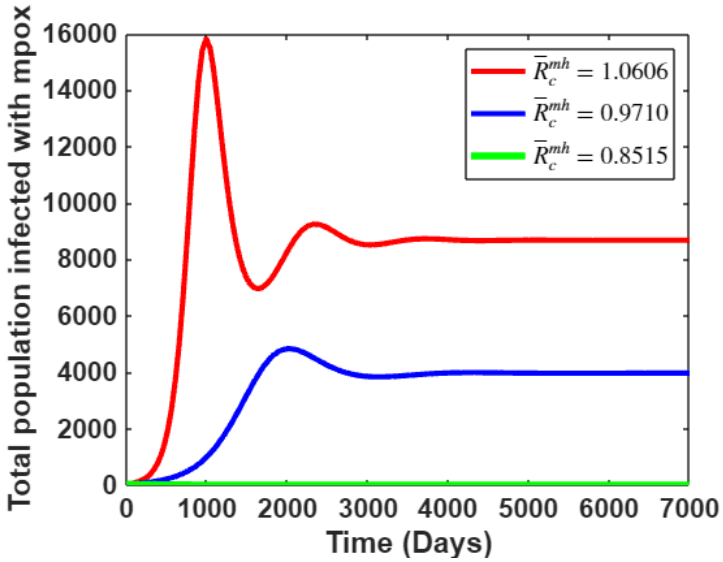

Figure 6. Numerical simulation. Simulation of the model (2.1) showing the total population of individuals infected with Mpox ($I_m + I_{hm} + I_{hm}^T$) over time for different values of the invasion reproduction number $\bar{\mathcal{R}}_c^{mh}$. The red curve ($\bar{\mathcal{R}}_c^{mh} = 1.0606$) shows a stable Mpox-endemic equilibrium when the Mpox invasion reproduction number $\bar{\mathcal{R}}_c^{mh} > 1$. The blue curve ($\bar{\mathcal{R}}_c^{mh} = 0.9710$) shows a stable Mpox-endemic equilibrium when $\bar{\mathcal{R}}_c^{mh} < 1$, and the green curve ($\bar{\mathcal{R}}_c^{mh} = 0.8515$) shows a stable Mpox-free equilibrium when $\bar{\mathcal{R}}_c^{mh} < 1$. Here, $\sigma = 1.8$ and $\sigma^T = 1.0$. The remaining parameter are given in Table 1.

Numerical simulations of the co-infection model (2.1) showing the total population of individuals infected with Mpox ($I_m + I_{hm} + I_{hm}^T$) over time is presented in Figure 6 for different values of the Mpox invasion reproduction number ($\bar{\mathcal{R}}_c^{mh}$). These simulations are used to confirm the existence of a backward bifurcation as revealed in our analysis. We used an initial total population $N(0) = 4\% \times CN_{pop}$, which corresponds to the MSM population in Canada at the beginning of the 2022-2023 Mpox outbreak (May 2022) [53], where $CN_{pop} = 38,929,902$, as defined in Table 1. The other initial conditions are set as follows: $E_m(0) = 43, I_m(0) = 25, I_h(0) = 15,795$, and $I_h^T(0) = 15,795$. Additionally, we assumed that there were no individuals in the rest of the model compartments at the beginning of the 2022 Mpox outbreak (compartments for individuals infected with Mpox), and we set the initial population

of susceptible $S(0) = N(0) - [E_m(0) + I_m(0) + I_h(0) + I_h^T(0)]$. The parameters used for these simulations are presented in Table 1, except otherwise stated in the figure caption. The values of $\bar{\mathcal{R}}_c^{mh}$ used in these simulations ($\bar{\mathcal{R}}_c^{mh} = 1.0606$, $\bar{\mathcal{R}}_c^{mh} = 0.9710$, and $\bar{\mathcal{R}}_c^{mh} = 0.8515$) were selected from the bifurcation diagram in the right panel of Figure 2, for $\sigma = 1.8$ and $\sigma^T = 1.0$, to show the model solution in different regions of the diagram. As predicted by our analysis, there is no Mpox-endemic solution in the system when $\bar{\mathcal{R}}_c^{mh} = 0.8515$ (green curve), which corresponds to having a stable Mpox-free equilibrium for this value of $\bar{\mathcal{R}}_c^{mh}$. In addition, there is a stable Mpox-endemic equilibrium for $\bar{\mathcal{R}}_c^{mh} = 0.9710$, which is less than one (blue curve). This confirms the existence of a backward bifurcation in the system, as the stable endemic equilibrium co-exists with the Mpox-free equilibrium. Lastly, we show the existence of the stable Mpox-endemic equilibrium for $\bar{\mathcal{R}}_c^{mh} = 1.060$, which is greater than one (red curve).

5. Discussion of results

The MSM population was extremely affected during the 2022 Mpox outbreak. Given that the MSM community is also adversely affected by HIV, it is imperative to understand the transmission of both diseases in the population. Recently, we developed a novel compartmental model [50] to study the co-interaction between HIV and Mpox in the MSM community. Specifically, this model was used to investigate the impact of HIV on the spread of Mpox within the MSM community through numerical simulations and a sensitivity analysis. Here, we studied the mathematical properties of the model. Specifically, we established the non-negativity and boundedness of the co-infection model. In addition, we performed bifurcation and stability analyses on the Mpox-free and Mpox-endemic equilibria of the model. Although only a few compartmental models have been proposed to investigate the co-interaction between Mpox and HIV [47–50], to the best of our knowledge, the stability analysis of equilibria for an endemic-invasive model for HIV and Mpox has not yet been investigated in the literature. Thus, we investigated this for the model developed in [50].

A local stability analysis of the Mpox-free equilibrium at an HIV-endemic regime revealed that the Mpox-free equilibrium of our model was locally asymptotically stable whenever the invasion reproduction number of Mpox $\mathcal{R}_c^{mh}$ was below 1 and unstable whenever $\mathcal{R}_c^{mh} > 1$. We established this using the Jacobian matrix of the system evaluated at the HIV endemic regime, and then applied the Routh-Hurwitz criterion for stability. This result is essential as it emphasizes that at an Mpox-free and HIV-endemic regime, with a little perturbation of the system around the Mpox-free equilibrium (which can be interpreted as the introduction of a few Mpox-infected individuals into a population that is completely susceptible to Mpox), will not lead to an Mpox outbreak as long as the invasion reproduction number of Mpox $\mathcal{R}_c^{mh}$ is below 1. However, Mpox will become endemic in the population whenever $\mathcal{R}_c^{mh} > 1$.

Next, we investigated the stability of the Mpox-endemic equilibrium at an HIV-endemic regime. Since only a few cases of Mpox-induced deaths were reported during the 2022 Mpox outbreak [71] and HIV treatments with ART significantly reduced deaths from HIV [36, 72], we considered a special case of our model where the disease-induced deaths for both Mpox and HIV were negligible. In other words, we set the Mpox and HIV death rates to zero in our model. Using the polynomial equation for the Mpox-endemic equilibrium, we obtained conditions under which positive solutions could exist. Particularly, we observed a scenario when two positive Mpox-endemic equilibria could exist when the Mpox invasion reproduction number was less than one, thus pointing towards the occurrence of a

backward bifurcation in the model. In addition, we showed that the backward bifurcation was due to the endemicity of HIV in the MSM population, and will not occur in a population where only Mpox is spreading. Numerical simulations of the co-infection model were used to verify our analysis.

Furthermore, we considered different scenarios to assess the effect of HIV on Mpox control. Our results were presented in terms of bifurcation diagrams. We considered potential scenarios whereby HIV infection could increase the susceptibility to Mpox, and found that the backward bifurcation lobe becomes larger as HIV-infected individuals became more susceptible to Mpox. This signifies that Mpox will become more difficult to control as HIV-infected individuals become more and more susceptible to Mpox due to a potential compromise in their immune system. To understand the effect of sexual contact on Mpox control, we varied the sexual contact rate while fixing all the remaining model parameters. We found that our co-infection model exhibited a transition from a forward bifurcation to a backward bifurcation as the sexual contact rate increased, which suggests that Mpox becomes more difficult to eradicate in the population as sexual contacts increases. In addition, it signifies that there is a critical sexual contact rate above which Mpox will be more difficult to eradicate in the population. Given the high level of sexual activities common among the MSM population [78, 79], it is important to investigate the effect of these activities on the control of Mpox in the population.

Lastly, we investigated the effect of HIV treatment on the control of Mpox. We computed the critical contact rate at which a backward bifurcation becomes a forward bifurcation, as the contact rate decreases, for different susceptibility levels to Mpox for HIV-infected individuals on ART. We found that the critical contact rate decreased as the susceptibility to Mpox increased. This result shows that sexual contact in the MSM population would need to be decreased for Mpox to be easily eradicated from the population, as the effectiveness of HIV treatment to reduce the susceptibility of HIV-infected individuals to Mpox decreases. In other words, as HIV-infected individuals on treatment become more susceptible to Mpox (treatment effectiveness decreases or individuals are increasingly not consistent with taken their medications), sexual contact would need to be decreased for Mpox to be easily controlled in the population. In other words, for the Mpox spread to be easily controlled, we need to ensure that the HIV treatment is effective enough to prevent those on treatment from having a higher vulnerability to Mpox (in other words, HIV-infected enrolled on ART consistently take their medications so as to prevent higher vulnerability to Mpox) if we want to maintain a high sexual contact rate in the MSM population.

6. Conclusions

Overall, our study investigated the potential detrimental effect of HIV endemicity on the control of Mpox in the MSM community using rigorous stability and bifurcation analyses. The study emphasizes the importance of HIV treatments and moderation in sexual activities on the control of Mpox spread within the MSM community. The results in this study will help inform public health officials and policymakers on interventions that could help facilitate the control of Mpox in the MSM population. A limitation of our study included considering only the MSM population instead of the entire population, which will enable a comprehensive understanding of the disease outbreak and interventions to implement and control the spread of Mpox in the entire population. With that said, considering only the MSM population is also a good idea since the majority of Mpox cases reported in the 2022 outbreak were in the MSM population (95%) [54, 80]. Another limitation of our study

involved using model parameters associated with the Canadian scenario of the 2022 Mpox outbreak. Although, this implies that our results are more aligned to Canada, the generalization of our modelling techniques and framework to other populations can easily be implemented, and our results can easily be used to infer the scenarios for other populations with a similar demography. We do not expect the results to differ much from those presented here. Additionally, parts of our analysis (endemic equilibrium analysis) did not consider an Mpox-induced mortality since only a very few Mpox-induced deaths were reported for the 2022 outbreak. However, studies on the current Clade 1b outbreak in Africa should incorporate Mpox-induced deaths due to the high mortality rate associated with this strain of the virus [23, 81]. A death rate of 5% for adults and up to 10% on average for children has been reported in DR Congo due to the Clade 1b Mpox outbreak [82, 83]. While the emergence of new Mpox clades and new patterns of transmission have been reported in recent outbreaks, they were not the focus of our current study, which is limited to the 2022-2023 outbreak scenario. In future studies, we plan to extend our model to incorporate these broader transmission routes and the more recent developments involving other clades. Additionally, we will investigate the co-interaction between HIV and Mpox beyond the MSM community. In addition, future studies will explore the global dynamics of an improved version of the model, using some novel techniques [84–87].

Use of AI tools declaration

The authors declare they have not used Artificial Intelligence (AI) tools in the creation of this article.

Funding statement

This research is funded by NSERC Discovery Grant (Grant No. RGPIN-2022-04559), NSERC Discovery Launch Supplement (Grant No: DGECR-2022-00454), New Frontier in Research Fund-Exploratory (Grant No. NFRFE-2021-00879), the Canadian Institute for Health Research (CIHR) under the Mpox and other zoonotic threats Team Grant (FRN. 187246), and Canada's International Development Research Centre (IDRC) (Grant No. 109981). W.A.W acknowledges financial support from the NSERC Discovery Grant (Appl No.: RGPIN-2023-05100).

Portions of this work were performed at the Los Alamos National Laboratory under the auspices of the US Department of Energy contract 89233218CNA000001 and supported by NIH grant R01-OD011095. W.A.W., J.D.K, and N.L.B. acknowledge financial support from the CIHR (FRN. 187246). N.L.B acknowledge funding from the European Union Horizon 2021 EUVABECO (grant 101132545). X.W. acknowledge funding support from NSERC of Canada (RGPIN-2020-06825 and DGECR-2020-00369) and the 2023-2026 National Natural Science Foundation of China (12271431).

Conflict of interest

The authors declare no conflict of interest.

Data availability

The MATLAB code used to generate the plots in the paper is available on GitHub at https://github.com/aomame2020/Mpox_HIV.

References

1. M. Patel, M. Adnan, A. Aldarhami, A. S. Bazaid, N. H. Saeedi, A. A. Alkayyal, et al., Current insights into diagnosis, prevention strategies, treatment, therapeutic targets, and challenges of monkeypox(Mpox) infections in human populations, *Life*, **13** (2023), 249. https://doi.org/10.3390/life13010249
2. J. Lu, H. Xing, C.Wang, M. Tang, C.Wu, F. Ye, et al., Mpox (formerly monkeypox): Pathogenesis, prevention, and treatment, *Signal Transduction Targeted Ther.*, **8** (2023), 458. https://doi.org/10.1038/s41392-023-01675-2
3. E. A. Falendysz, J. G. Lopera, T. E. Rocke, J. E. Osorio, Monkeypox virus in animals: Current knowledge of viral transmission and pathogenesis in wild animal reservoirs and captive animal models, *Viruses*, **15** (2003), 905. https://doi.org/10.3390/v15040905
4. N. Kumar, A. Acharya, H. E. Gendelman, S. N. Byrareddy, The 2022 outbreak and the pathobiology of the monkeypox virus, *J. Autoimmun.*, **131** (2022), 102855. https://doi.org/10.1016/j.jaut.2022.102855
5. J. G. Breman, Kalisa-Ruti, M. V. Steniowski, E. Zanotto, A. I. Gromyko, I. Arita, Human monkeypox, 1970–1979, 1980. Available from: https://iris.who.int/handle/10665/67095.
6. D. L. Heymann, M. Szczeniowski, K. Esteves, Re-emergence of monkeypox in africa: A review of the past six years, *British Med. Bull.*, **54** (1998), 693–702. https://doi.org/10.1093/oxfordjournals.bmb.a011720
7. H. Nilasari, M. Trifitriana, R. Anadya, L. Ameline, D. Pratiwi, The evolving monkeypox outbreak amongst homosexual and bisexual transmission: A systematic review, *J. Pakistan Assoc. Dermat.*, **34** (2024), 243–254. https://www.jpad.com.pk/index.php/jpad/article/view/2502
8. A. M. McCollum, V. Shelus, A. Hill, T. Traore, B. Onoja, Y. Nakazawa, et al., Epidemiology of human mpox—worldwide, 2018–2021, *MMWR Morb. Mortal. Wkly. Rep.*, **72** (2023), 68–72. http://dx.doi.org/10.15585/mmwr.mm7203a4
9. M. G. Reynolds, I. K. Damon, Outbreaks of human monkeypox after cessation of smallpox vaccination, *Trends Microbiol.*, **20** (2012), 80–87. https://doi.org/10.1016/j.tim.2011.12.001
10. G. M. Zaucha, P. B. Jahrling, T. W. Geisbert, J. R. Swearengen, L. Hensley, The pathology of experimental aerosolized monkeypox virus infection in cynomolgus monkeys (macaca fascicularis), *Lab. Invest.*, **81** (2001), 1581–1600. https://doi.org/10.1038/labinvest.3780373
11. J. Kaler, A. Hussain, G. Flores, S. Kheiri, D. Desrosiers, Monkeypox: A comprehensive review of transmission, pathogenesis, and manifestation, *Cureus*, **14** (2022). https://doi.org/10.7759/cureus.26531

12. P. Kumar, B. Chaudhary, N. Yadav, S. Devi, A. Pareek, S. Alla, et al., Recent advances in research and management of human monkeypox virus: An emerging global health threat, *Viruses*, **15** (2023), 937. https://doi.org/10.3390/v15040937

13. K. Mellou, K. Tryfinopoulou, S. Pappa, K. Gkolfinopoulou, S. Papanikou, G. Papadopoulou, et. al., Overview of Mpox outbreak in Greece in 2022–2023: Is it over, *Viruses*, **15** (2023), 1384. https://doi.org/10.3390/v15061384

14. S. T. Al Awaidy, F. Khamis, M. Sallam, R. M. Ghazy, H. Zaraket, Monkeypox (Mpox) outbreak: More queries posed as cases soar globally, *Sultan Qaboos Univ. Med. J.*, **23** (2023), 1–4. https://doi.org/10.18295/squmj.8.2022.046

15. L. T. Allan-Blitz, M. Gandhi, P. Adamson, I. Park, G. Bolan, J. D. Klausner, A position statement on mpox as a sexually transmitted disease, *Clin. Infect. Dis.*, **76** (2013), 1508–1512. https://doi.org/10.1093/cid/ciac960

16. RR Assessment, Monkeypox multi-country outbreak, *Eur. Cent. Dis. Prev. Control*, **2022** (2022).

17. B. Ortiz-Saavedra, E. S. Montes-Madariaga, C. Cabanillas-Ramirez, N. Alva, A. Ricardo-Martinez, D. A. Leon-Figueroa, et al., Epidemiologic situation of HIV and monkeypox coinfection: A systematic review, *Vaccines*, **11** (2023), 246. https://doi.org/10.3390/vaccines11020246

18. S. Cahill, Lessons learned from the us public health response to the 2022 mpox outbreak, *LGBT Health*, **10** (2023), 489–495. https://doi.org/10.1089/lgbt.2022.0274

19. K. K. Kota, J. Hong, C. Zelaya, A. P. Riser, A. Rodriguez, D. L. Weller, et al., Racial and ethnic disparities in mpox cases and vaccination among adult males—united states, may-december 2022, *MMWR Morb. Mortal. Wkly. Rep.*, **72** (2023), 398–403. http://dx.doi.org/10.15585/mmwr.mm7215a4

20. H. Sachdeva, R. Shahin, S. Ota, S. Isabel, C. S. Mangat, R. Stuart, et al., Preparing for mpox resurgence: Surveillance lessons from outbreaks in toronto, canada, *J. Infect. Dis.*, **229** (2024), S305–S312. https://doi.org/10.1093/infdis/jiad533

21. A. Zebardast, T. Latifi, N. Jandaghi, M. G. Barzoki, S. Malekshahi, Plausible reasons for the resurgence of mpox (formerly monkeypox): An overview, *Trop. Dis., Travel Med. Vaccines*, **9** (2023), 23 https://doi.org/10.1186/s40794-023-00209-6

22. S. Mohanto, M. Faiyazuddin, A. D. Gholap, D. Jogi, A. Bhunia, K. Subbaram, et al., Addressing the resurgence of global monkeypox (Mpox) through advanced drug delivery platforms, *Travel Med. Infect. Dis.*, **56** (2023), 102636. https://doi.org/10.1016/j.tmaid.2023.102636

23. L. M. Masirika, A. Kumar, M. Dutt, A. T. Ostadgavahi, B. Hewins, N. M. Bubala, et. al., Complete genome sequencing, annotation, and mutational profiling of the novel clade I human Mpox virus, Kamituga strain, *J. Infect. Dev. Ctries*, **18** (2024), 600–608. https://doi.org/10.3855/jidc.20136

24. E. Alakunle, D. Kolawole, D. Diaz-Canova, F. Alele, O. Adegboye, U. Moens, et al., A comprehensive review of monkeypox virus and Mpox characteristics, *Front. Cell. Infect. Microbiol.*, **14** (2024), 1360586. https://doi.org/10.3389/fcimb.2024.1360586

25. L. Taylor, Mpox in Africa: WHO and Africa CDC consider declaring public health emergency as cases spike, *British Med. J.*, **386** (2024). https://doi.org/10.1136/bmj.q1795

26. World Health Organization, WHO director-general declares Mpox outbreak a public health emergency of international concern, 2024.
27. Kaiser Family Foundation, Black Americans and HIV/AIDS: The basics, 2023.
28. Global statistics, 2024. Available from: https://www.hiv.gov/hiv-basics/overview/data-and-trends/global-statistics.
29. Global HIV AIDS statistics—Fact sheet, 2024. Available from: https://www.unaids.org/en/resources/fact-sheet.
30. H. Swinkels, A. J. Vaillant, A. Nguyen, P. Gulick. HIV and AIDS. *StatPearls*, (2024). Available from: https://www.ncbi.nlm.nih.gov/books/NBK534860/.
31. Centers for Disease Control and Prevention, How HIV spreads, 2023. Available from: https://www.cdc.gov/hiv/causes/index.html.
32. Q. Tollett, S. Safdar, A. B. Gumel, Dynamics of a two-group model for assessing the impacts of pre-exposure prophylaxis, testing and risk behaviour change on the spread and control of HIV/AIDS in an MSM population, *Infect. Dis. Modell.*, **9** (2024), 103–127. https://doi.org/10.1016/j.idm.2023.11.004
33. D. Patel, C. H. Johnson, A. Krueger, B. Maciak, L. Belcher, N. Harris, et al., Trends in HIV testing among US adults, aged 18-64 years, 2011–2017, *AIDS Behav.*, **24** (2020), 532–539. https://doi.org/10.1007/s10461-019-02689-0
34. S. J. Challacombe, Global inequalities in HIV infection, *Oral Dis.*, **26** (2020), 16–21. https://doi.org/10.1111/odi.13386
35. A. T. Boyd, I. Oboho, H. Paulin, H. Ali, C. Godfrey, A. Date, et al., Addressing advanced HIV disease and mortality in global HIV programming, *AIDS Res. Ther.*, **17** (2020), 1–7. https://doi.org/10.1186/s12981-020-00296-x
36. Statista, *Death rate for human immunodeficiency virus (HIV) in Canada from 2000 to 2022*, 2024.
37. Common conditions and diseases in HIV-positive men who have sex with men, 2024. Available from: https://www.ohtn.on.ca/rapid-response-82-conditions-diseases-hiv-positive-gay-men.
38. O. Mitja, A. Alemany, M. Marks, J. Mora, J. Rodríguez-Aldama, M. Silva, et. al., Mpox in people with advanced HIV infection: A global case series, *The Lancet*, **401** (2023), 939–949. https://doi.org/10.1016/S0140-6736(23)00273-8
39. O. Mitja, D. Ogoina, B. K. Titanji, C. Galvan, J-J Muyembe, M. Marks, et al., Monkeypox, *The Lancet*, **401** (2023), 60–74. https://doi.org/10.1016/S0140-6736(22)02075-X
40. Centers for Disease Control and Prevention, *CDC health advisory; severe manifestations of monkeypox among people who are immunocompromised due to HIV or other conditions*, 2023. Available from: https://emergency.cdc.gov/han/2022/pdf/CDC_HAN_475.pdf.
41. Centers for disease control and prevention, *Clinical considerations for treatment and prophylaxis of mpox infection in people who are immunocompromised*, 2023. Available from: https://www.cdc.gov/poxvirus/mpox/clinicians/people-with-HIV.html.
42. J. Elford, G. Hart, If HIV prevention works, why are rates of high-risk sexual behavior increasing among MSM, *AIDS Educ. Prev.*, **15** (2003), 294–308. https://doi.org/10.1521/aeap.15.5.294.23825

43. W. Thienkrua, F. van Griensven, P. A. Mock, E. F. Dunne, B. Raengsakulrach, W. Wimonsate, et al., Young men who have sex with men at high risk for HIV, Bangkok MSM cohort study, Thailand 2006–2014, *AIDS Behav.*, **22** (2018), 2137–2146. https://doi.org/10.1007/s10461-017-1963-7

44. S. K. Sulaiman, F. Isma'il Tsiga-Ahmed, M. S. Musa, B. T. Makama, A. K. Sulaiman, T. B. Abdulaziz, Global prevalence and correlates of Mpox vaccine acceptance and uptake: A systematic review and meta-analysis, *Commun. Med.*, **4** (2024), 136. https://doi.org/10.1038/s43856-024-00564-1

45. R. A. Ghaffar, S. Shahnoor, M. Farooq, Increased prevalence of HIV among monkeypox patients–an alarming update, *New Microbes New Infect.*, **49-50** (2022), 101039. https://doi.org/10.1016/j.nmni.2022.101039

46. J. Kowalski, I. Cielniak, E. Garbacz-Łagożna, G. Cholewińska-Szymańska, M. Parczewski, Comparison of clinical course of mpox among HIV-negative and HIV-positive patients: A 2022 cohort of hospitalized patients in central Europe, *J. Med. Virol.*, **95** (2023), e29172. https://doi.org/10.1002/jmv.29172

47. C. P. Bhunu, S. Mushayabasa, J. M. Hyman, Modelling HIV/AIDS and monkeypox co-infection. *Appl. Math. Comput.*, **218** (2012), 9504–9518. https://doi.org/10.1016/j.amc.2012.03.042

48. O. I. Marcus, A. Augustine, T. Jonathan, A co-infection model for monkeypox and HIV/AIDS: Sensitivity and bifurcation analyses, *J. Scient. Res. Rep.*, **30** (2024), 351–368. https://doi.org/10.9734/jsrr/2024/v30i51951

49. O. O. Peace, O. A. Godwin, B. Bolaji, A compartmental deterministic epidemiological model with non-linear differential equations for analyzing the co-infection dynamics between COVID-19, HIV, and monkeypox diseases, *Healthcare Anal.*, (2024), 100311. https://doi.org/10.1016/j.health.2024.100311

50. A. Omame, Q. Han, S. A. Iyaniwura, E. Adeniyi, N. L. Bragazzi, X. Wang, et al., Understanding the impact of HIV on mpox transmission in an MSM population: A mathematical modeling study, *Infect. Dis. Modell.*, **9** (2024), 1117–1137. https://doi.org/10.1016/j.idm.2024.05.008

51. M. S. Cohen, Y. Q. Chen, M. McCauley, T. Gamble, M. C. Hosseinipour, N. Kumarasamy, et al., Prevention of HIV-1 infection with early antiretroviral therapy, *N. Engl. J. Med.*, **365** (2011), 493–505. https://doi.org/10.1056/NEJMoa1105243

52. R. W. Eisinger, C. W. Dieffenbach, A. S. Fauci, HIV viral load and transmissibility of HIV infection, *JAMA*, **321** (2019), 451–452. https://doi.org/10.1001/jama.2018.21167

53. World Bank Group, Population, total-Canada, 2023. Available from: https://data.worldbank.org/indicator/SP.POP.TOTL?locations=CA.

54. N. L. Bragazzi, Q. Han, S. A. Iyaniwura, A. Omame, A. Shausan, X. Wang, et al., Adaptive changes in sexual behavior in the high-risk population in response to human monkeypox transmission in canada can help control the outbreak: Insights from a two-group, two-route epidemic model, *J. Med. Virol.*, **95** (2023), e28575. https://doi.org/10.1002/jmv.28575

55. M. Xiridou, F. Miura, P. Adam, E. Op de Coul, J. de Wit, J. Wallinga, The fading of the mpox outbreak among men who have sex with men: A mathematical modelling study, *J. Infect. Dis.*, (2023), e121–e130. https://doi.org/10.1093/infdis/jiad414

56. E. Beer, V. B. Rao, A systematic review of the epidemiology of human monkeypox outbreaks and implications for outbreak strategy, *PLoS Negl. Trop. Dis.*, **13** (2019), e0007791. https://doi.org/10.1371/journal.pntd.0007791

57. F. Miura, C. E. van Ewijk, J. A. Backer, M. Xiridou, E. Franz, E. Op de Coul, et al., Estimated incubation period for monkeypox cases confirmed in the Netherlands, May 2022, *Eurosurveillance*, **27** (2022), 2200448. https://doi.org/10.2807/1560-7917.ES.2022.27.24.2200448

58. I. H. Spicknall, E. D. Pollock, P. A. Clay, A. M. Oster, K. Charniga, N. Masters, et al., Modeling the impact of sexual networks in the transmission of monkeypox virus among gay, bisexual, and other men who have sex with men—United States, 2022, *Morb. Mortal. Wkly. Rep.*, **71** (2022), 1131–1135.

59. V. D. Lima, J. Zhu, K. G. Card, N. J. Lachowsky, G. Chowell-Puente, Z. Wu, et al., Can the combination of TasP and PreP eliminate HIV among MSM in British Columbia, Canada, *Epidemics*, **35** (2021), 100461. https://doi.org/10.1016/j.epidem.2021.100461

60. Y. Shen, C. Zhang, M. A. Valimaki, H. Qian, L. Mohammadi, Y. Chi, et al., Why do men who have sex with men practice condomless sex? A systematic review and meta-synthesis, *BMC Infect. Dis.*, **22** (2022), 850. https://doi.org/10.1186/s12879-022-07843-z

61. Z. Mukandavire, K. Bowa, W. Garira, Modelling circumcision and condom use as HIV/AIDS preventive control strategies, *Math. Comput. Modell.*, **46** (2007), 1353–1372. https://doi.org/10.1016/j.mcm.2007.01.001

62. D. R. MacFadden, D. H. Tan, S. Mishra, Optimizing HIV pre-exposure prophylaxis implementation among men who have sex with men in a large urban centre: A dynamic modelling study, *J. Int. AIDS Soc.*, **19** (2016), 20791. https://doi.org/10.7448/IAS.19.1.20791

63. Centers for Disease Control and Prevention, *Impact of monkeypox outbreak on select behaviors*, 2023. Available from: https://www.cdc.gov/poxvirus/monkeypox/response/2022/amis-select-behaviors.html.

64. P. van den Driessche, J. Watmough, Reproduction numbers and sub-threshold endemic equilibria for compartmental models of disease transmission, *Math. Biosci.*, **180** (2002), 29–48. https://doi.org/10.1016/S0025-5564(02)00108-6

65. E. J. Routh, *A treatise on the stability of a given state of motion, particularly steady motion: being the essay to which the Adams prize was adjudged in 1877, in the University of Cambridge*. Macmillan and Company, 1877.

66. F. J. Kraus, M. Mansour, M. Sebek, Hurwitz matrix for polynomial matrices, in *Stability Theory: Hurwitz Centenary Conference Centro Stefano Franscini, Ascona, 1995*, Springer, (1996), 67–74.

67. O. C. Collins, K. J. Duffy, Dynamics and control of mpox disease using two modelling approaches, *Model. Earth Syst. Environ.*, **10** (2024), 1657–1669. https://doi.org/10.1007/s40808-023-01862-8

68. M. M. Al-Shomrani, S. S. Musa, A. Yusuf, Unfolding the transmission dynamics of monkeypox virus: An epidemiological modelling analysis, *Mathematics*, **11** (2023), 1121. https://doi.org/10.3390/math11051121

69. L. Wang, Global dynamical analysis of hiv models with treatments, *Int. J. Bifurcation Chaos*, **22** (2012), 1250227. https://doi.org/10.1142/S0218127412502276

70. Z. Mukandavire, P. Das, C. Chiyaka, F. Nyabadza, Global analysis of an HIV/AIDS epidemic model, *World J. modelling and simulation*, **6** (2010), 231–240.

71. Public Health Agency of Canada, *Epidemiological summary report: 2022-23 Mpox outbreak in Canada*, 2024.

72. E. Slaymaker, J. Todd, M. Marston, C. Calvert, D. Michael, J. Nakiyingi-Miiro, et al., How have ART treatment programmes changed the patterns of excess mortality in people living with HIV? estimates from four countries in East and Southern Africa, *Global Health Action*, **7** (2014). https://doi.org/10.3402/gha.v7.22789

73. MathWorks, Matlab r2024a, 2024. Available from: https://matlab.mathworks.com.

74. C. Castillo-Chavez, B. Song, Dynamical models of tuberculosis and their applications, *Math. Biosci. Eng.*, **1** (2004), 361–404. https://doi.org/10.3934/mbe.2004.1.361

75. A. B. Gumel, Causes of backward bifurcations in some epidemiological models, *J. Math. Anal. Appl.*, **395** (2012), 355–365. https://doi.org/10.1016/j.jmaa.2012.04.077

76. B. Anderson, J. Jackson, M. Sitharam, Descartes' rule of signs revisited, *Am. Math, Mon.*, **105** (1998), 447–451. https://doi.org/10.1080/00029890.1998.12004907

77. B. J. Turner, Adherence to antiretroviral therapy by human immunodeficiency virus—infected patients, *J. Infect. Dis.*, **185** (2002), S143–S151. https://doi.org/10.1038/s41598-018-21081-x

78. C. C. Hoff, D. Chakravarty, S. C. Beougher, T. B. Neilands, L. A. Darbes, Relationship characteristics associated with sexual risk behavior among MSM in committed relationships, *AIDS Patient Care STDs*, **26** (2012), 738–745. https://doi.org/10.1089/apc.2012.0198

79. B. R. Simon Rosser, K. J. Horvath, L. A. Hatfield, J. L. Peterson, S. Jacoby, A. Stately, et al., Predictors of HIV disclosure to secondary partners and sexual risk behavior among a high-risk sample of HIV-positive MSM: Results from six epicenters in the US, *AIDS care*, **20** (2008), 925–930. https://doi.org/10.1080/09540120701767265

80. D. Ogoina, M. Iroezindu, H. I. James, R. Oladokun, A. Yinka-Ogunleye, P. Wakama, et al., Clinical course and outcome of human monkeypox in Nigeria, *Clin. Infect. Dis.*, **71** (2020), e210–e214. https://doi.org/10.1093/cid/ciaa143

81. M. A. Zinnah, M. B. Uddin, T. Hasan, S. Das, F. Khatun, M. H. Hasan, et al., The re-emergence of mpox: Old illness, modern challenges, *Biomedicines*, **12** (2024), 1457. https://doi.org/10.3390/biomedicines12071457

82. E. H. Vakaniaki, C. Kacita, E. Kinganda-Lusamaki, A. O'Toole, T. Wawina-Bokalanga, D. Mukadi-Bamuleka, et al., Sustained human outbreak of a new MPXV clade I lineage in the Eastern Democratic Republic of the Congo, *Nat. Med.*, **30** (2024), 2791–2795. https://doi.org/10.1038/s41591-024-03130-3

83. D. A. Schwartz, High rates of miscarriage and stillbirth among pregnant women with clade I Mpox(monkeypox) are confirmed during 2023–2024 DR Congo outbreak in South Kivu Province, *Viruses*, **16** (2024), 1123. https://doi.org/10.3390/v16071123

84. L. Zhang, M. ur Rahman, M. Arfan, A. Ali, Investigation of mathematical model of transmission co-infection TB in HIV community with a non-singular kernel, *Results Phys.*, **28** (2021), 104559. https://doi.org/10.1016/j.rinp.2021.104559

85. N. Mohankumar, L. Rajagopal, J. J. Nieto, Optimal control for co-infection with COVID-19-associated pulmonary aspergillosis in icu patients with environmental contamination, *Math. Biosci. Eng.*, **20** (2023), 9861–9875. https://doi.org/10.3934/mbe.2023432

86. C. J. Silva, C. Cruz, D. F. M. Torres, A. P. Munuzuri, A. Carballosa, I. Area, et al., Optimal control of the COVID-19 pandemic: Controlled sanitary deconfinement in Portugal, *Sci. Rep.*, **11** (2021), 3451. https://doi.org/10.1038/s41598-021-83075-6

87. B. Li, Z. Eskandari, Dynamical analysis of a discrete-time SIR epidemic model, *J. Franklin Inst.*, **360** (2023), 7989–8007. https://doi.org/10.1016/j.jfranklin.2023.06.006

88. C. Mitchell, C. Kribs, Invasion reproductive numbers for periodic epidemic models, *Infect. Dis. Modell.*, **4** (2019), 124–141. https://doi.org/10.1016/j.idm.2019.04.002

A. Appendix

In this section, we provide detailed proofs to some important results stated within the main manuscript.

A.1. Mpox submodel

The Mpox submodel is obtained from the co-infection model (2.1) by setting the variables related to HIV and co-infection dynamics ($I_h, I_h^T, E_{hm}, I_{hm}, R_{hm}, E_{hm}^T, I_{hm}^T$, and R_{hm}^T) to zero. The model is applicable to a scenario where only Mpox is introduced and is spreading in a population. The equations are given by the following:

$$\begin{aligned}
\frac{\mathrm{d}S}{\mathrm{d}t} &= \Lambda - \lambda_{ms} S - \mu S,\\
\frac{\mathrm{d}E_m}{\mathrm{d}t} &= \lambda_{ms} S - (\alpha + \mu) E_m,\\
\frac{\mathrm{d}I_m}{\mathrm{d}t} &= \alpha E_m - (\gamma + \delta_m + \mu) I_m,\\
\frac{\mathrm{d}R_m}{\mathrm{d}t} &= \gamma I_m - \mu R_m,
\end{aligned} \tag{A.1}$$

where λ_{ms} is the force of infection given by the following:

$$\lambda_{ms} = \frac{c\, p_m (1 - \nu\varepsilon) I_m}{S + E_m + I_m + R_m}.$$

We derive the control reproduction number for the Mpox submodel (A.1) using the next-generation matrix approach. The matrix $\mathcal{F}_m$, which describes the new infections and matrix $\mathcal{V}_m$ which describes

all other transitions within the infectious stages of the model are defined as follows:

$$\mathcal{F}_m = \begin{pmatrix} \frac{c\, p_m(1-\nu\varepsilon)I_m}{S+E_m+I_m+R_m} S \\ \\ 0 \end{pmatrix}, \qquad \mathcal{V}_m = \begin{pmatrix} (\alpha+\mu)\, E_m \\ \\ (\gamma+\delta_m+\mu)I_m - \alpha E_m \end{pmatrix}$$

Taking the partial derivatives of $\mathcal{F}_m$ and $\mathcal{V}_m$ with respect to the disease classes E_m and I_m and evaluating at the disease free equilibrium $\Psi_{0m} = \left(\frac{\Lambda}{\mu}, 0, 0, 0\right)$, we have the following:

$$F_m = \begin{pmatrix} 0 & c\, p_m(1-\nu\varepsilon) \\ \\ 0 & 0 \end{pmatrix}, \qquad V_m = \begin{pmatrix} (\alpha+\mu) & 0 \\ \\ -\alpha & (\gamma+\delta_m+\mu) \end{pmatrix}$$

Thus, the control reproduction number for the Mpox submodel is given by the following:

$$\mathcal{R}_c^m = \rho\left(F_m V_m^{-1}\right) = \frac{c\, p_m(1-\nu\varepsilon)\alpha}{(\alpha+\mu)(\gamma+\delta_m+\mu)}. \tag{A.2}$$

The endemic equilibrium of the Mpox submodel (A.1) is defined by the following:

$$\Psi_{em} = \left(S^*, E_m^*, I_m^*, R_m^*\right),$$

where the equilibrium points S^*, E_m^*, I_m^*, and R_m^* are given by the following:

$$\begin{aligned} S^* &= \frac{\Lambda}{\lambda_{ms}^e + \mu}, \qquad E_m^* = \frac{\Lambda\lambda_{ms}^e}{(\alpha+\mu)(\lambda_{ms}^e+\mu)}, \qquad I_m^* = \frac{\alpha\,\Lambda\,\lambda_{ms}^e}{(\alpha+\mu)\,(\gamma+\delta_m+\mu)(\lambda_{ms}^e+\mu)}, \\ R_m^* &= \frac{\alpha\,\gamma\,\Lambda\,\lambda_{ms}^e}{\mu\,(\alpha+\mu)\,(\gamma+\delta_m+\mu)(\lambda_{ms}^e+\mu)} \end{aligned} \tag{A.3}$$

where the force of infection at the endemic equilibrium is as follows:

$$\lambda_{ms}^e = \frac{\mu\,(\alpha+\mu)\,(\gamma+\delta_m+\mu)\,\left(\mathcal{R}_c^m - 1\right)}{\mu\,(\gamma+\delta_m+\mu) + \alpha\,(\gamma+\mu)}, \tag{A.4}$$

and $\mathcal{R}_c^m$ is the control reproduction number for the Mpox submodel, which is defined in (A.2).

The polynomial equation associated with the endemic equilibrium of the Mpox submodel is given by the following:

$$\left[\mu\,(\gamma+\delta_m+\mu) + \alpha\,(\gamma+\mu)\right]\lambda_{ms}^e + \mu\,(\alpha+\mu)(\gamma+\delta_m+\mu)\left(1-\mathcal{R}_c^m\right) = 0, \tag{A.5}$$

where λ_{ms}^e is the force of infection for Mpox at the endemic equilibrium. It can be easily observed that Eq (A.5) has no sign changes whenever $\mathcal{R}_c^m < 1$, thus completely ruling out the possibility of a backward bifurcation in the Mpox submodel. However, Eq (A.5) has one sign change whenever $\mathcal{R}_c^m > 1$, thus pointing towards the existence of a forward bifurcation in the Mpox submodel.

A.2. HIV submodel (Mpox free model)

In this section, the HIV submodel, which corresponds to the Mpox free model is obtained from the co-infection model (2.1). This is derived by setting the variables related to Mpox and co-infection dynamics
($E_m, I_m, R_m, E_{hm}, I_{hm}, R_{hm}, E_{hm}^T, I_{hm}^T$, and R_{hm}^T) to zero. This model describes the dynamics of HIV in the population when there is no Mpox. Its equations are as follows:

$$\begin{aligned}
\frac{\mathrm{d}S}{\mathrm{d}t} &= \Lambda - \lambda_{hs} S - \mu S, \\
\frac{\mathrm{d}I_h}{\mathrm{d}t} &= \lambda_{hs} S - (\tau + \delta_h + \mu) I_h, \\
\frac{\mathrm{d}I_h^T}{\mathrm{d}t} &= \tau I_h - \left(\delta_h^T + \mu\right) I_h^T
\end{aligned} \tag{A.6}$$

where λ_{hs} is the force of infection for this model given by the following:

$$\lambda_{hs} = \frac{c\, p_h (1 - \nu\varepsilon)(I_h + \eta I_h^T)}{S + I_h + I_h^T}.$$

Next, we compute the control reproduction number for the HIV submodel (A.6) following a similar approach used in Section A.1. In this case, the matrix $\mathcal{F}_h$ and $\mathcal{V}_h$ are defined as follows:

$$\mathcal{F}_h = \begin{pmatrix} \frac{c\, p_h (1-\nu\varepsilon)(I_h + \eta I_h^T)}{S + I_h + I_h^T} S \\ \\ 0 \end{pmatrix}, \qquad \mathcal{V}_h = \begin{pmatrix} (\tau + \delta_h + \mu) I_h \\ \\ (\delta_h^T + \mu) I_h^T - \tau I_h \end{pmatrix}$$

Taking the partial derivatives of $\mathcal{F}_h$ and $\mathcal{V}_h$ with respect to the disease classes I_h and I_h^T and evaluating at the disease free equilibrium $\Psi_{0h} = \left(\frac{\Lambda}{\mu}, 0, 0\right)$, we have the following:

$$F_h = \begin{pmatrix} c\, p_h (1 - \nu\varepsilon) & \eta c\, p_h (1 - \nu\varepsilon) \\ \\ 0 & 0 \end{pmatrix}, \qquad V_h = \begin{pmatrix} (\tau + \delta_h + \mu) & 0 \\ \\ -\tau & (\delta_h^T + \mu) \end{pmatrix}$$

Thus, the control reproduction number for the HIV submodel is given by the following:

$$\mathcal{R}_c^h = \rho\left(F_h V_h^{-1}\right) = \frac{c\, p_h (1 - \nu\varepsilon)}{(\tau + \delta_h + \mu)} + \frac{\eta\, c\, p_h (1 - \nu\varepsilon)\tau}{(\tau + \delta_h + \mu)(\delta_h^T + \mu)}, \tag{A.7}$$

The endemic equilibrium of the HIV submodel (A.6) is defined by the following:

$$\Psi_{eh} = \left(S^*, I_h^*, I_h^{T*}\right),$$

where the equilibrium points S^*, I_h^*, and I_h^{T*} are given by the following:

$$S^* = \frac{\Lambda(\delta_h^T + \mu + \tau)}{\Upsilon\left(\mathcal{R}_c^h - 1\right) + \mu\chi}, \qquad I_h^* = \frac{\Lambda(\delta_h^T + \mu)\left(\mathcal{R}_c^h - 1\right)}{\Upsilon\left(\mathcal{R}_c^h - 1\right) + \mu, \chi}, \qquad I_h^{T*} = \frac{\Lambda\tau\left(\mathcal{R}_c^h - 1\right)}{\Upsilon\left(\mathcal{R}_c^h - 1\right) + \mu\chi}, \tag{A.8}$$

where $\Upsilon = (\tau + \delta_h + \mu)(\delta_h^T + \mu)$. Here, $\mathcal{R}_c^h$ is the control reproduction number for the HIV submodel, defined in (A.7).

The polynomial equation associated with the endemic equilibrium of the HIV submodel is given by the following:

$$\left(\delta_h^T + \tau + \mu\right)\lambda_{hs}^e + (\tau + \delta_h + \mu)(\delta_h^T + \mu)\left(1 - \mathcal{R}_c^h\right) = 0, \tag{A.9}$$

where λ_{hs}^e is the force of infection for HIV at the endemic equilibrium. It can be easily observed that Eq (A.9) has no sign changes whenever $\mathcal{R}_c^h < 1$, thus completely ruling out the possibility of a backward bifurcation in the HIV submodel. However, the equation has one sign change whenever $\mathcal{R}_c^h > 1$, thus pointing towards the existence of a forward bifurcation in the HIV submodel.

A.3. Mpox submodel at the HIV endemic regime

In this section, we present the Mpox submodel at the HIV endemic regime. This is derived from the main model (2.1) by replacing the HIV associated variables I_h and I_h^T with their corresponding solutions at the HIV endemic regime, that is I_h^* and I_h^{T*}, respectively. The associated equations are given by the following:

$$\begin{aligned}
\frac{\mathrm{d}S}{\mathrm{d}t} &= \Lambda - \lambda_m S - \mu S,\\
\frac{\mathrm{d}E_m}{\mathrm{d}t} &= \lambda_m S - (\alpha + \mu)\, E_m,\\
\frac{\mathrm{d}I_m}{\mathrm{d}t} &= \alpha E_m - (\gamma + \mu + \delta_m) I_m,\\
\frac{\mathrm{d}R_m}{\mathrm{d}t} &= \gamma I_m - \mu R_m,\\
\\
\frac{\mathrm{d}E_{hm}}{\mathrm{d}t} &= \lambda_{hm} I_h^* - (\tau + \alpha + \delta_h + \mu)\, E_{hm},\\
\frac{\mathrm{d}I_{hm}}{\mathrm{d}t} &= \alpha E_{hm} - (\gamma + \rho\,\tau + \delta_{hm} + \mu)\, I_{hm},\\
\frac{\mathrm{d}R_{hm}}{\mathrm{d}t} &= \gamma I_{hm} - (\tau + \delta_h + \mu)\, R_{hm},\\
\frac{\mathrm{d}E_{hm}^T}{\mathrm{d}t} &= \lambda_{hm}^T\, I_h^{T*} + \tau E_{hm} - \left(\alpha + \delta_h^T + \mu\right) E_{hm}^T,\\
\frac{\mathrm{d}I_{hm}^T}{\mathrm{d}t} &= \alpha E_{hm}^T + \rho\,\tau I_{hm} - \left(\gamma + \delta_{hm}^T + \mu\right) I_{hm}^T,\\
\frac{\mathrm{d}R_{hm}^T}{\mathrm{d}t} &= \gamma I_{hm}^T + \tau\, R_{hm} - (\delta_h^T + \mu)\, R_{hm}^T,
\end{aligned} \tag{A.10}$$

where I_h^*, and I_h^{T*} are given by the following:

$$I_h^* = \frac{\Lambda(\delta_h^T + \mu)\left(\mathcal{R}_c^h - 1\right)}{\mho}, \qquad I_h^{T*} = \frac{\tau\Lambda\left(\mathcal{R}_c^h - 1\right)}{\mho}. \tag{A.11}$$

Here, $\mho = \varphi_h(\delta_h^T + \mu)\left(\mathcal{R}_c^h - 1\right) + \mu\chi$ with $\varphi_h = \tau + \delta_h + \mu$, $\chi = \delta_h^T + \mu + \tau$, and $\mathcal{R}_c^h$ is the HIV associated control reproduction number, which is greater than one for the HIV endemic regime to exist. It is given by the following:

$$\mathcal{R}_c^h = \frac{\Upsilon_h}{\varphi_h}\left(1 + \frac{\eta\,\tau}{\delta_h^T + \mu}\right), \tag{A.12}$$

where $\Upsilon_h = c\,p_h(1 - \nu\varepsilon)$.

Lemma A.1. *[88] Suppose there exists a disease model, where $\mathcal{A}$ is the set of resident pathogens and $\mathcal{A}_c$ is the set of invading pathogens. Assume that all the reproductive numbers in the $\mathcal{A}$-only subsystem exceed 1. If x_0 is an $\mathcal{A}_c$-infection free equilibrium of the model, then x_0 is locally asymptotically stable if ${}_{\mathcal{A}}\tilde{R}_0 < 1$, but unstable if ${}_{\mathcal{A}}\tilde{R}_0 > 1$, where ${}_{\mathcal{A}}\tilde{R}_0$ is the overall invasion reproduction number (IRN) when all pathogens in A are resident.*